Acid- and Base-Catalyzed Decomposition of Acetaldehyde Hydrate and Hemiacetals in Aqueous Solution[1]

Poul E. Sørensen*[2] and William P. Jencks*

Contribution No. 1619 from the Graduate Department of Biochemistry, Brandeis University, Waltham, Massachusetts 02554. Received January 7, 1987

Abstract: Rate constants and structure–reactivity parameters for general acid and general base catalysis of the reactions of acetaldehyde with water and alcohols at 25 °C and ionic strength 1.0 (KCl) were determined by trapping the carbonyl group formed upon cleavage of acetaldehyde hydrate or hemiacetal with semicarbazide or hydrazine. The Brønsted coefficients of $\alpha = 0.50$–0.59 for general acid catalysis by a class e mechanism are larger than those for the corresponding reactions with formaldehyde. The difference is described by a normalized interaction coefficient $p_{xy} = 0.067 = \partial\alpha/-\partial\sigma = \partial\rho/\partial pK_{HB}$. The increase in α with decreasing pK_a of the alcohol is described by the coefficient $p_{xy} = 0.020 = \partial\alpha/-\partial pK_{lg} = \partial\beta_{lg}/-\partial pK_{HB}$. A small increase in β_{lg} for the acetaldehyde compared with formaldehyde reactions corresponds to a normalized coefficient $p_{yy'} = 0.014 = \partial\beta_{lg}/-\partial\sigma = \partial\rho/-\partial pK_{lg}$. These coefficients are consistent with a concerted reaction mechanism and a largely diagonal reaction coordinate on an energy contour diagram that is defined by the structure–reactivity parameters; there may be a larger vertical than horizontal component to the reaction coordinate. A stepwise mechanism is excluded by a requirement for rate constants that would have to be in the range 10^{13}–10^{18} s^{-1} for proton transfer and for decomposition of the dipolar addition species $R^{\pm}$. Extrapolated rate constants for the cleavage of $R^{\pm}$ in the range 10^{20}–10^{23} s^{-1} suggest that the concerted mechanism is enforced by the absence of a significant lifetime for $R^{\pm}$. The general base catalyzed reactions show a decrease in β_{lg} and an increase in β for acetaldehyde compared with formaldehyde that correspond to normalized values of $p_{yy'} = -0.052 = \partial\beta_{lg}/-\partial\sigma = \partial\rho/-\partial pK_{lg}$ and $p_{xy} = 0.042 = \partial\beta/-\partial\sigma = \partial\rho/-\partial pK_{BH}$. The increase in Brønsted β values with decreasing pK_a of the leaving group and the increase in β_{lg} with decreasing catalyst pK_a are described by an interaction coefficient $p_{xy'} = 0.07 = \partial\beta/-\partial pK_{lg} = \partial\beta_{lg}/-\partial pK_{BH}$, and upward curvature in the dependence of log k on the pK_a of the leaving group (an "anti-Hammond effect") is described by a value of $p_y = -0.20 = \partial\beta_{lg}/-\partial pK_{lg}$. These interaction coefficients and a value of $p_x = 0 = \partial\beta/-\partial pK_{BH}$ from the linear Brønsted plots correspond to a reaction coordinate that is rotated 57° clockwise from the vertical on an energy contour diagram that is defined by the structure–reactivity parameters, with β for proton transfer on the x axis. The results support a fully concerted reaction mechanism with an important component of proton transfer in the transition state. Rate constants for the "water-catalyzed" reaction are consistent with those for buffer bases; there is no evidence for a cyclic mechanism involving proton transfer through water. Hydroxide ion catalysis of the reaction represents specific base catalysis. The equilibrium constant for acetaldehyde hydration was found to be $K_h = 1.2 \pm 0.1$ at 25 °C, ionic strength 1.0.

We report here an examination of the mechanisms of general acid and general base catalysis of the reactions of water and alcohols with acetaldehyde. These two mechanisms of catalysis are entirely different and are discussed separately; however, the work is described in a single long paper for economy of presentation of the experimental data. Catalysis of the addition of water, alcohols, and other nucleophiles to the carbonyl group, one of the most basic and widespread reactions in chemistry and biochemistry, usually involves the transfer of protons between an acid or base catalyst and the carbonyl oxygen atom or the nucleophile. The hydration and other addition reactions of acetaldehyde serve as a prototype for this class of reactions.[3,4] Several kinetically equivalent mechanisms are possible for these reactions.[5,6]

General acid catalysis of carbonyl addition reactions has been shown to follow a sequence of mechanisms that depend on the stability of the initially formed addition intermediate.[4] Strongly basic oxygen and thiol anions add without significant acid catalysis, the addition of less basic thiol anions is catalyzed by diffusion-controlled trapping of the anionic addition compound, R^-, and the addition of still less basic thiol anions is catalyzed by hydrogen bonding to the acid catalyst in a preassociation mechanism. It has been suggested that the addition of still weaker nucleophiles, such as RSH and ROH, occurs with a fully concerted mechanism of general acid catalysis.[4,7]

The estimated lifetime of the dipolar addition intermediate, $R^{\pm}$, that is required for a stepwise mechanism of addition of water and alcohols to formaldehyde and structure–reactivity correlations supports a concerted class e mechanism for general acid catalysis of this reaction, in which the catalyst interacts with the electrophilic carbonyl group (eq 1), but a stepwise pathway was not excluded conclusively.[7-9] We describe here an examination of the corresponding reactions of acetaldehyde that was undertaken with the goal of obtaining a definitive answer to the question of whether the mechanism is concerted. Acetaldehyde is a more stable electrophile that will give a less stable dipolar intermediate, $R^{\pm}$. The α value of 0.5 for the hydration of acetaldehyde[3] already suggests a concerted mechanism for general acid catalysis. The results show that the reaction is concerted because the rate constants that would be required for a stepwise mechanism are too large to permit reaction through an intermediate with a significant lifetime. Furthermore, extrapolation of the rate constants for cleavage of other addition compounds suggests that the concerted mechanism is enforced because $R^{\pm}$, even if it could be formed,

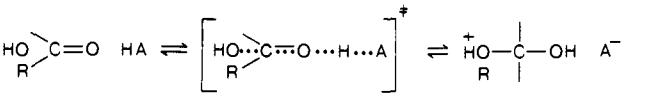

(1)

(1) This paper is dedicated to R. P. Bell on the occasion of his 80th birthday and in appreciation of his many contributions to our present understanding of mechanisms in acid–base catalysis. This research was supported in part by grants from the National Institutes of Health (GM 20888), the National Science Foundation (PCM 81-17816), and H. C. Orsteds Rejselegat for Pharmaceuter. Preliminary results were presented at the Seventh IUPAC Conference on Physical Organic Chemistry, Auckland, New Zealand, August 20–24, 1984 (P.E.S.).

(2) Chemistry Department A, The Technical University of Denmark, DK-2800, Lyngby, Denmark.

(3) Bell, R. P.; Rand, M. H.; Wynne-Jones, K. M. A. *Trans. Faraday Soc.* **1956**, *52*, 1093.

(4) Gilbert, H. F.; Jencks, W. P. *J. Am. Chem. Soc.* **1977**, *99*, 7931.

(5) Jencks, W. P. *Prog. Phys. Org. Chem.* **1964**, *2*, 63. Bell, R. P. *Adv. Phys. Org. Chem.* **1966**, *4*, 1.

(6) Jencks, W. P. *Acc. Chem. Res.* **1976**, *9*, 425.

(7) Funderburk, L. H.; Aldwin, W. P.; Jencks, W. P. *J. Am. Chem. Soc.* **1978**, *100*, 5444.

(8) McClelland, R. A.; Coe, M. *J. Am. Chem. Soc.* **1983**, *105*, 2718. The p_{xy} coefficient was normalized by $\rho_{equib} = 1.7$; $p_{xy} = 0.06/1.7 = 0.035$.

(9) Stewart, R. *Can. J. Chem.* **1984**, *62*, 907.

0002-7863/87/1509-4675$01.50/0

does not have a sufficient lifetime to exist as an intermediate.

General base catalysis of the corresponding reactions of formaldehyde hydrate and hemiacetals proceeds by a class n mechanism (eq 2), in which the catalyst removes a proton from the attacking nucleophilic reagent in the addition direction and protonates the leaving group in the reverse direction. This mechanism is followed

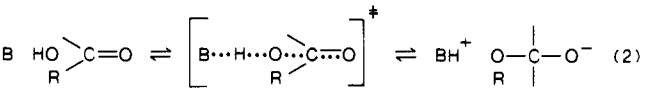

(2)

for a large number of hydrolysis and other reactions that involve the attack of ROH on electrophilic carbon centers or the generation of such centers by ROH removal.[6-8,10-17] These reactions are convenient to study in the direction of decomposition of the hydrate or hemiacetal by trapping the aldehyde with a carbonyl reagent. We describe here an examination of the cleavage of acetaldehyde derivatives which extends the previously reported structure–reactivity data for formaldehyde derivatives[7] by changing the electrophilic reagent, as well as ROH and the catalyst. McClelland and Coe have examined the effect of substituents on the electrophilic reagent for the hydration of substituted benzaldehydes,[8] and a study of the secondary deuterium isotope effects for catalysis of the cleavage of formaldehyde hemiacetals has provided information on the amount of C–O bond cleavage in the transition states of these reactions.[18]

It was concluded from this work that the data are consistent with a concerted class n mechanism in which changes in both C–O bonding and proton transfer occur in the transition state.[7,18] The results can be described by a diagonal reaction coordinate on an energy contour diagram that is defined by the observed structure–reactivity parameters.[19,20] They can also be described by an energy contour diagram that is defined directly by the energies of the reactants and the products of the partial reactions, assuming a diagonal reaction coordinate.[21] This description differs somewhat from proposals that the proton rests in an almost symmetrical double minimum energy well in the transition state[22] and that the reaction occurs by sequential uncoupled changes in C–O bond length, followed by proton transfer and further changes in C–O bond length.[23,24]

The experiments reported here demonstrate the changes in structure–reactivity parameters with changing structure of the electrophilic reagent that are predicted for a fully concerted, coupled mechanism and provide additional evidence consistent with this mechanism.

Experimental Section

Materials. Acetaldehyde (Aldrich 99+%) was distilled in a current of nitrogen and fractions were collected in dry ice. Samples of approximately 2 mL were kept in sealed vials at −20 °C. Dehydrated ethyl alcohol was used without further purification. Methanol, 2,2-dichloroethanol, 2-methoxyethanol, and methoxyacetic acid were distilled before use, the 2-methoxyethanol under nitrogen. Trifluoroethanol was distilled over anhydrous calcium sulfate and sodium bicarbonate.[25] 2-Chloroethanol was distilled over anhydrous calcium sulfate after neutralization with anhydrous sodium carbonate (pH paper); the fraction boiling at 128 °C was collected.[26] Trifluoroethanol and 2-dichloroethanol were stored in sealed vessels at −20 °C. Semicarbazide hydrochloride, hydrazine monohydrochloride, potassium acetate, cyanoacetic acid, chloroacetic acid, 3-chloropropionic acid, and cacodylic acid were recrystallized before use. Succinic acid and inorganic compounds were of certified purity. Glass-distilled water was used throughout.

Equilibria. Hemiacetals were formed by injecting 10 μL of cooled acetaldehyde into 100 μL of each alcohol (or water to form the hydrate). The solutions were kept at −20 °C (aqueous solutions at 0 °C), which enhances the degree of reaction ($\Delta H < 0$). The solutions are stable at this temperature except that acidic alcohols give biphasic kinetics after 1–2 days, presumably because of acetal formation.[7] A rough estimate of the amount of hemiacetal formation was obtained by measuring the change in absorbance at 278 nm, $A_0 - A_\infty$, when an aliquot of a few microliters of acetaldehyde (50% v/v in acetonitrile) was injected into an alcohol. The dimensionless equilibrium constant for the addition reaction was estimated from $K_{add} = (A_0 - A_\infty)/A_\infty$, where A_0 was obtained by extrapolation to $t = 0$.

The equilibrium constant for hydration was determined from the ratio of the rate constants in the two directions, $K_h = k_h/k_d$. The sum of the hydration and dehydration rate constants, $k_h + k_d$, was obtained spectrophotometrically from the first-order kinetic plots resulting from injecting samples of acetaldehyde (in acetonitrile) into buffers. Alternatively, a simple "temperature-jump" technique was useful: from a solution of acetaldehyde in buffer equilibrated at 0 °C, a 2.5-mL sample was quickly transferred to a water-jacketed spectrophotometer cell thermostated with circulating water at 25 °C; the temperature of the sample in such a cell reaches 25 °C within 20–30 s and the approach to the new equilibrium was followed spectrophotometrically to provide a value for $(k_h + k_d)$. The dehydration rate constant, k_d, was obtained in the same buffer by the trapping technique that is described in the next paragraph. Succinate buffers (pH 6.2) are preferred, since at this pH the rate of the water-catalyzed reaction is at a minimum.

Kinetics. Trapping experiments were carried out at 25 °C with the ionic strength maintained at 1.0 (KCl) throughout. The trapping reagents used were semicarbazide ($pK_a = 3.86$) at pH <6.2 and hydrazine ($pK_a = 8.26$) at pH >6.2.[7,27,28] Increases in absorbance, due to acetaldehyde hydrazone formation and indicating the breakdown rates of hemiacetal or hydrate, were followed spectrophotometrically at 240 nm. Reactions were initiated by injecting a few microliters of the hemiacetal- or hydrate-containing solutions described above into 2.5 mL of a mixture of buffer and the trapping reagent. The concentration of trapping reagent was in the range 0.001–0.020 M, depending on pH and the overall rate of reaction, which is low enough for catalysis to be negligible. Generally, the "trapping capacity" of the trapping reagents was adequate at such concentrations. This was checked regularly by changing the concentration of the reagent; such changes have no effect on the measured rate constants.

Typical absorbance vs. time plots for methyl, ethyl, and methoxyethyl hemiacetal breakdown were first-order throughout, with $A \sim 0$ at $t = 0$, and $A = A_\infty$ at $t = \infty$, and the rate constant, k_{obsd}, was obtained from a plot of ln $(A_\infty - A)$ against time. However, for the remaining alcohols and for water a burst is seen in the beginning of the reaction due to the presence of free acetaldehyde that reacts instantaneously with the trapping reagent.

The rate constants for decomposition of the acetaldehyde adducts were obtained from a first-order plot of the change in absorbance after this burst. Only ~20% of the acetaldehyde is converted into hemiacetal at equilibrium in trifluoroethanol at −20 °C. Consequently, the burst is large, the first-order change in absorbance is relatively small, and the rate constants for this compound are less accurate than those for the other substrates.

Breakdown rates were measured for at least three buffer ratios per catalyst. First-order rate constants, k_{obsd}, were determined in duplicate at six different buffer concentrations in the range 0.05–0.50 M for each buffer ratio. Plots of k_{obsd} against total buffer concentration are linear within experimental error, and values of k_{cat} and k_0 were obtained from the slopes and intercepts of the lines. Values of the buffer-independent rate constant, k_0, at high pH were determined in dilute hydrazine buffers. In acidic solution, k_0 was determined in solutions adjusted to a desired pH with HCl.

(10) Fife, T. H. *Acc. Chem. Res.* **1972**, *58* 264–272.
(11) Gravitz, N.; Jencks, W. P. *J. Am. Chem. Soc.* **1974**, *96*, 507.
(12) Ta-Shma, R.; Jencks, W. P. *J. Am. Chem. Soc.* **1986**, *108*, 8040.
(13) Bernasconi, C. F.; Gandler, J. R. *J. Am. Chem. Soc.* **1978**, *100*, 8117.
(14) Jensen, J. L.; Herold, L. R.; Lenz, P. A.; Trusty, S.; Sergi, V.; Bell, K.; Rogers, P. *J. Am. Chem. Soc.* **1979**, *101*, 4672.
(15) Gilbert, H. F.; Jencks, W. P. *J. Am. Chem. Soc.*, **1982**, *104*, 6769.
(16) Richard, J. P.; Jencks, W. P. *J. Am. Chem. Soc.*, **1984**, *106*, 1396.
(17) Gandler, J. R. *J. Am. Chem. Soc.* **1985**, *107*, 8218–8223.
(18) Palmer, J. L.; Jencks, W. P. *J. Am. Chem. Soc.*, **1980**, *102*, 6472.
(19) Jencks, D. A.; Jencks, W. P. *J. Am. Chem. Soc.* **1977**, *99*, 7948.
(20) Jencks, W. P. *Chem. Rev.* **1985**, *85*, 511–527.
(21) Grunwald, E. *J. Am. Chem. Soc.* **1985**, *107*, 4710–4715.
(22) Eliason, E.; Kreevoy, M. M. *J. Am. Chem. Soc.* **1978**, *100*, 7037.
(23) Guthrie, J. P. *J. Am. Chem. Soc.* **1980**, *102*, 5286.
(24) Lamaty, G.; Menut, C. *Pure Appl. Chem.* **1982**, *54*, 1837. Lamaty, G.; Menut, C. *Recl. Trav. Chim. Pays-Bas* **1984**, *103*, 54.
(25) Ballinger, P.; Long, F. A. *J. Am. Chem. Soc.* **1959**, *81*, 1050. Ballinger, P.; Long, F. A. *J. Am. Chem. Soc.* **1960**, *82*, 795.
(26) Bednar, R. A.; Colman, R. F. *J. Protein Chem.* **1982**, *1*, 203.
(27) (a) Bell, R. P.; Evans, P. G. *Proc. R. Soc. London, Ser. A* **1966**, *291*, 297. (b) Gruen, L. C.; Mc Tigue, P. T. *J. Chem. Soc.* **1963**, 5224. Kurz, J. L. *J. Am. Chem. Soc.* **1967**, *89*, 3524. Kurz, J. L.; Coburn, J. F. *J. Am. Chem. Soc.* **1967**, *89*, 3528. Greenzaid, P.; Luz, Z.; Samuel, D. *J. Am. Chem. Soc.* **1967**, *89*, 756. Ahrens, M.-L.; Strehlow, H. *Discuss. Faraday Soc.* **1965**, *39*, 112.
(28) (a) Evans, P. G.; Miller, G. R.; Kreevoy, M. M. *J. Phys. Chem.* **1965**, *69*, 4325. (b) Koehler, K.; Sandstrom, W.; Cordes, E. H. *J. Am. Chem. Soc.* **1964**, *86*, 2413.

Table I. Experimental Values of K_{add} = $[CH_3CH(OH)OR]/[CH_3CHO]$ for the Reaction of Acetaldehyde with Various Hydroxylic Solvents, ROH, at 25 °C[a]

R	pK_{ROH}[b] in water	K_{add}[c,u]	method
CH_3CH_2	16	>10	UV
H	15.74	1.23 (16), 1.17 (11)	UV (kinetic)[d]
		1.54,[e] 1.22,[f] 1.22[g]	UV
		0.93,[h] 1.20,[i] 1.20[j]	
		1.06,[k] 0.85,[l] 1.06[m]	
		1.49,[n] 1.23,[o] 1.23[p]	NMR
		1.22,[q] 1.28,[r] 1.06[k]	
		1.49,[s]	UV (kinetic)[t]
CH_3	15.54	>10	UV
$CH_3O(CH_2)_2$	14.82	>10	UV
$Cl(CH_2)_2$	14.31	>1	UV
Cl_2CHCH_2	12.89	≈1	UV
F_3CCH_2	12.37	~0.2	UV

[a] Literature values reported at other temperatures have been corrected to 25 °C by using a ΔH value of −21.32 kJ mol.[f] [b] Reference 25. [c] Quantitative studies are only carried out for ROH = HOH where $K_{add} = K_h$. [d] $K_{add} = K_h = k_h/k_d$ where $(k_h + k_d)$ and k_d are determined separately (see text). [e] Rumpf, P.; Bloch, C. *Compt. Rend.* **1951**, *233*, 1364. [f] Bell, R. P.; Clunie, J. C. *Trans. Faraday Soc.* **1952**, *48*, 439. [g] Edwards, J. O.; Ibne-Rasa, K. M.; Choi, E. I.; Rice, C. L. *J. Phys. Chem.* **1962**, *66*, 1212. [h] Gruen, L. C.; McTigue, P. T. *J. Chem. Soc.* **1963**, 5217. [i] Buschmann, H.-J.; Dutkiewicz, E.; Knoche, W. *Ber. Bunsenges. Phys. Chem.* **1982**, *86*, 129. [j] Lewis, C. A., Jr.; Wolfenden, R. *J. Am. Chem. Soc.* **1973**, *95*, 6685. [k] Pocker, Y.; Meany, J. E. *J. Phys. Chem.* **1967**, *71*, 3113. [l] Lienhard, G. E.; Jencks, W. P. *J. Am. Chem. Soc.* **1966**, *88*, 3982. [m] Kurz, J. L. *J. Am. Chem. Soc.* **1967**, *89*, 3524. [n] Lombardi, E.; Sogo, P. B. *J. Chem. Phys.* **1960**, *32*, 635. [o] Fujiwara, Y.; Fujiwara, S. *Bull. Chem. Soc. Jpn.* **1963**, *36*, 574. [p] Reference 28a. [q] Ahrens, M.-L.; Strehlow, H. *Discuss. Faraday Soc.* **1965**, *39*, 112. [r] Lewis, C. A., Jr.; Wolfenden, R. *Biochemistry* **1977**, *16*, 4886. [s] Reference 27a. [t] $K_h = (A_\infty - A_0)/A_0$ determined by trapping.[27a] [u] Numbers in parentheses are standard deviations.

Results

Equilibria. Some experimental values of the equilibrium constant, K_{add}, for the formation of the hydrate and hemiacetals of acetaldehyde in water and various alcohols are given in Table I. The qualitative nature of these data is obvious apart from the case where ROH is water.

The equilibrium constant for the hydration of acetaldehyde, K_h, is of special interest. The literature provides a long list of K_h values obtained by different procedures at many different temperatures, but there is a striking disagreement between these constants, even if only post-1950 reports of K_h at 25 °C are considered (Table I). The first of our experimental values for this solvent, $K_{add} = K_h = 1.23$ (16), is derived from kinetic runs in acetate buffer (0.2 M, 15% acid, $I = 1.0$ (KCl)): an average of nine determinations of $(k_h + k_d)$ for approach to equilibrium gave 5.8 (5) × 10^{-2} s^{-1} for this sum by applying the injection method described in the Experimental Section. The numbers in parentheses are standard deviations. An average of 2.61 (6) × 10^{-2} s^{-1} was found from six single experimental values of k_d in the same buffer by trapping with semicarbazide. Our second K_h value in Table I, $K_h = 1.17$ (9), was obtained in succinate buffer (0.02 M, pH 6.2, $I = 1.0$ (KCl): five determinations of $(k_h + k_d)$ by the "temperature-jump" method gave an average of 1.42 (4) × 10^{-2} s^{-1} for this constant. Trapping of acetaldehyde in the same buffer, using semicarbazide or hydrazine, resulted in k_d = 0.665 (30) × 10^{-2} s^{-1}. A closer look at the origin of the more extreme estimates of K_h by various authors in Table I points to the application of procedures or assumptions that may be uncertain or doubtful in some cases. We suggest that $K_h = 1.2$ (1) is the most likely estimate of this constant at 25 °C, $I = 1.0$.

Kinetics. In the following we present results from our systematic kinetic studies of the acid- and base-catalyzed decomposition of the various acetaldehyde hemiacetals and the hydrate. The buffer-independent rate constants k_0 obtained from the intercepts of plots of observed pseudo-first-order rate constants (k_{obsd}) against buffer concentration are given in Table II. The numbers in parentheses are standard deviations. These rate constants depend upon pH in the usual characteristic way (Figure 1). The second-order rate constants k_w for water catalysis, k_H for catalysis by the proton, and k_{HO} for catalysis by hydroxide ion were obtained from the slopes and intercepts of plots of k_0 against hydrogen ion and hydroxide ion activities, respectively, based on observed pH values (Table II, Figure 2).

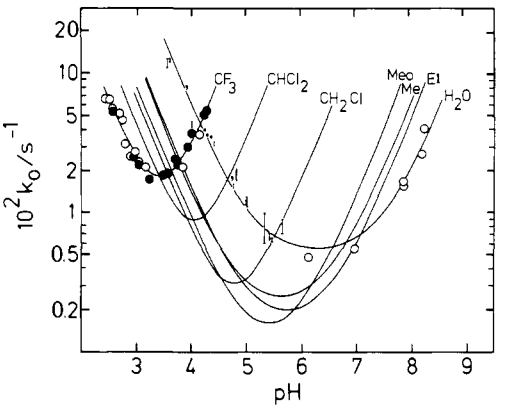

Figure 1. Buffer-independent rate constants as a function of pH for cleavage of acetaldehyde hydrate (H_2O), ethyl hemiacetal (Et), methyl hemiacetal (Me), methoxyethyl hemiacetal (MeO), 2-chloroethyl hemiacetal (CH_2Cl), 2,2'-dichloroethyl hemiacetal ($CHCl_2$), and trifluoroethyl hemiacetal (CF_3) at ionic strength 1.0 (KCl) and 25 °C (Table II). Experimental points are shown only for the hydrate and trifluoroethyl hemiacetal. Closed circles and error bars are from experiments in buffers, open circles are from measurements in unbuffered solution. The curves are drawn from $k_0 = k_w + k_H a_{H^+} + k_{HO} a_{HO^-}$ (Table II).

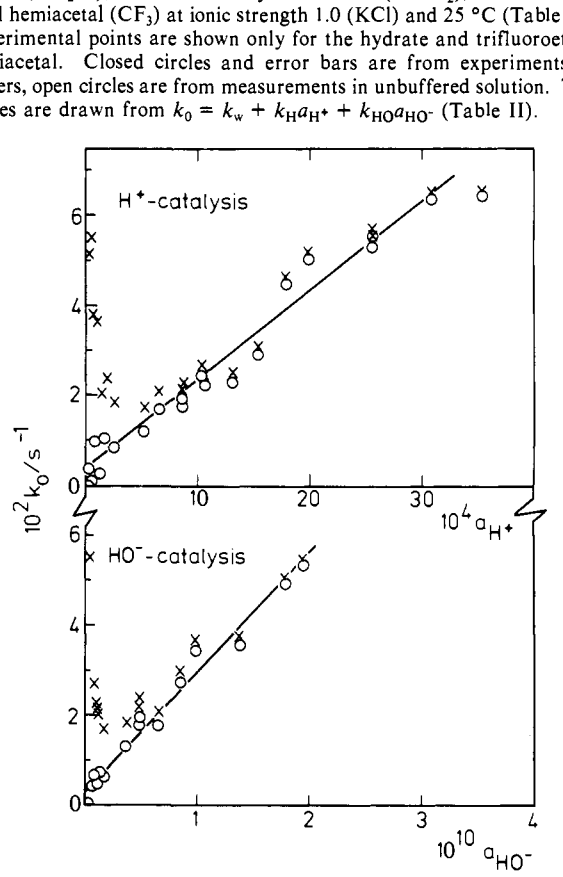

Figure 2. Plots for the determination of k_H, k_{HO}, and k_w (Table II) for the decomposition of acetaldehyde trifluoroethyl hemiacetal. Experimental values (X); values corrected for catalysis by H^+ or HO^- (O).

The open circles in Figure 2 show plots of k_0 for the decomposition of acetaldehyde trifluoroethyl hemiacetal against a_{H^+} and against a_{HO^-} that were corrected for catalysis by HO^- and H^+, respectively; the corrections become large for the points close to the origin. The values of k_w in Table II are less accurate than those for reactions of formaldehyde[7] because of a higher sensitivity of the acetaldehyde reactions to acid and base catalysis, which gives larger values of α and β. The values of k_w vary from 20% of k_0 for the trifluoroethyl hemiacetal to approximately 90% for the hydrate.

Table II. Kinetic Data for the Acid- and Base-Catalyzed Breakdown of Acetaldehyde Hydrate and Hemiacetals, $CH_3CH(OH)OR \rightarrow CH_3CHO + ROH$, at 25 °C and Ionic Strength 1.0 (KCl)

cat[g]	fraction acid	pH	10^2k_{cat}/ M^{-1} s^{-1}	$10^2k_0/s^{-1}$	10^2k_{HB}/ M^{-1} s^{-1}	10^2k_B/ M^{-1} s^{-1}	cat[g]	fraction acid	pH	10^2k_{cat}/ M^{-1} s^{-1}	$10^2k_0/s^{-1}$	10^2k_{HB}/ M^{-1} s^{-1}	10^2k_B/ M^{-1} s^{-1}
					ROH = CH_3CH_2OH (pK = 16)[a]								
1	0.001	5.27	0.22 (4)	0.47 (1)			4	0.010	6.04	0.82 (4)	0.227 (6)	18 (1)	0.6 (2)
	0.010	4.23	1.35 (8)	0.90 (2)	100 (10)	0.12 (4)		0.100	4.98	2.0 (1)	0.33 (3)[b]		
	0.050	3.57	4.7 (5)	4.20 (5)				0.250	4.49	6.0 (1)	0.62 (2)[b]		
	0.100	3.26	10.5 (9)	8.0 (2)				0.500	3.97	9.5 (6)	1.6 (1)[b]		
2	0.010	4.75	1.00 (5)	0.43 (2)	74 (5)	0.3 (1)		0.750	3.47	14 (1)	5.1 (2)[b]		
	0.050	4.00	4.40 (5)	1.6 (1)			5	0.150	5.32	3.2 (1)	0.18 (2)	6.2 (2)	2.4 (2)
	0.100	3.70	7.4 (7)	3.3 (1)				0.350	4.82	3.5 (2)	0.40 (4)		
3	0.010	5.52	0.78 (3)	0.160 (5)[b]	27 (3)	0.5 (1)		0.650	4.28	5.0 (2)	0.90 (2)		
	0.100	4.43	3.5 (4)	0.67 (2)[b]			6	0.500	6.17	7.9 (5)	0.25 (5)	12 (1)	4.3 (5)
	0.250	3.95	6.5 (2)	1.72 (4)[b]				0.750	5.65	6.5 (5)	0.17 (5)		
	0.400	3.61	11.3 (1)	3.70 (5)[b]				0.900	4.98	4.9 (2)	0.29 (5)		
					k_H = 145 (3) M^{-1} s^{-1},[c] k_{HO} = 4.7 (3) × 10^4 M^{-1} s^{-1},[d] k_w = 0.15 (5) × 10^{-2}/55.5 M^{-1} s^{-1}								
					ROH = H_2O (pK = 15.74)[a]								
1	0.001	5.27	0.8 (2)	1.85 (3)	390 (15)	0.4 (2)	4	0.010	6.06	3.41 (5)	0.48 (2)	69 (4)	2.8 (2)
	0.010	4.23	3.5 (3)	4.0 (1)				0.050	5.42	5.4 (3)	0.68 (4)		
	0.025	3.91	10.2 (6)	8.1 (3)				0.100	5.00	8.5 (1)	1.16 (4)		
	0.050	3.57		12 (1)			5	0.150	5.32	9.1 (9)	0.8 (2)	29 (2)	5.0 (5)
2	0.010	4.75	3.1 (2)	1.75 (5)	180 (10)	1.4 (2)		0.350	4.82	12.8 (1)	1.9 (2)		
	0.025	4.36	6.1 (3)	3.5 (1)				0.650	4.28	21 (1)	3.7 (1)		
	0.050	4.00	10.0 (5)	4.4 (2)				0.900	3.61	31 (4)	12.5 (3)		
3	0.010	5.46	2.63 (2)	0.64 (2)	100 (5)	1.6 (2)	6	0.500	6.17	19 (2)	0.5 (1)	18 (2)	20 (2)
	0.050	4.77	6.5 (3)	1.56 (4)				0.750	5.65	19 (2)	0.8 (1)		
	0.100	4.41	11.6 (9)	3.2 (1)				0.900	4.99	18 (2)	1.2 (1)		
					k_H = 570 (30) M^{-1} s^{-1},[c] k_{HO} = 1.7 (1) × 10^4 M^{-1} s^{-1},[d] k_w = 0.5 (1) × 10^{-2}/55.5 M^{-1} s^{-1}								
					ROH = CH_3OH (pK = 15.54)[a]								
1	0.001	5.27	0.40 (4)	0.61 (2)	90 (10)	0.34 (4)	4	0.001	6.04	1.5 (1)	0.35 (1)	15 (2)	1.5 (1)
	0.010	4.23	1.4 (1)	0.88 (2)				0.100	4.98	3.04 (4)	0.35 (2)[b]		
	0.050	3.57	4.7 (3)	3.9 (1)				0.250	4.49	5.3 (1)	0.62 (2)[b]		
	0.100	3.26	9.5 (5)	7.2 (2)				0.500	3.97	8.8 (4)	1.5 (1)[b]		
2	0.010	4.75	1.07 (5)	0.44 (2)	67 (5)	0.4 (1)		0.750	3.47	11 (1)	4.7 (1)[b]		
	0.050	4.00	3.9 (1)	1.5 (1)			5	0.150	5.32	4.42 (7)	0.27 (2)	5.4 (2)	4.2 (1)
	0.100	3.70	6.9 (1)	2.9 (1)				0.350	4.82	4.51 (5)	0.38 (2)		
3	0.010	5.52	1.02 (9)	0.25 (1)[b]	28 (3)	0.8 (1)		0.650	4.28	4.99 (5)	0.80 (4)		
	0.100	4.43	3.82 (6)	0.62 (2)[b]			6	0.500	6.17	13 (1)	0.4 (1)	6.2 (3)	21 (1)
	0.250	3.95	7.1 (1)	1.65 (5)[b]				0.750	5.65	10.5 (2)	0.25 (2)		
	0.400	3.61	11.8 (1)	3.45 (5)[b]				0.900	4.98	7.1 (3)	0.25 (2)		
					k_H = 130 (3) M^{-1} s^{-1},[c] k_{HO} = 6.4 (1) × 10^4 M^{-1} s^{-1},[d] k_w = 0.20 (2) × 10^{-2}/55.5 M^{-1} s^{-1}								
					ROH = $CH_3OCH_2CH_2OH$ (pK = 14.82)[a]								
1	0.010	4.23	0.72 (2)	0.56 (2)	50 (5)	0.25 (5)	4	0.001	6.04	0.73 (7)	0.23 (2)[b]	7.6 (6)	0.7 (1)
	0.050	3.57	2.7 (2)	2.5 (1)				0.100	4.98	1.42 (3)	0.23 (1)[b]		
	0.100	3.26	5.1 (3)	4.80 (5)				0.250	4.49	2.5 (1)	0.42 (2)[b]		
2	0.010	4.75	0.4 (1)	0.30 (2)	41 (1)	(0.10 (5))		0.500	3.97	4.3 (3)	1.0 (1)[b]		
	0.050	4.00	2.1 (2)	1.1 (1)				0.750	3.47	5.9 (5)	3.0 (1)[b]		
	0.100	3.70	4.1 (1)	1.85 (5)				0.900	3.01	6 (2)	8.5 (5)[b]		
	0.250	3.06	10.4 (4)	7.7 (1)			5	0.150	5.32	1.93 (6)	0.14 (1)	2.44 (8)	1.85 (5)
3	0.010	5.52	0.54 (4)	0.146 (3)	14 (2)	0.4 (1)		0.350	4.82	2.07 (4)	0.21 (2)		
	0.100	4.43	1.76 (6)	0.50 (2)[b]				0.650	4.28	2.23 (8)	0.65 (5)		
	0.250	3.95	3.6 (3)	1.05 (5)[b]				0.900	3.61		3.2 (2)		
	0.400	3.61	6.5 (1)	2.20 (5)[b]			6	0.500	6.17	6.1 (2)	0.32 (2)	1.9 (1)	10.5 (5)
								0.750	5.65	4.12 (5)	0.16 (2)		
								0.900	4.99	2.56 (2)	0.18 (2)		
					k_H = 87 (2) M^{-1} s^{-1},[c] k_{HO} = 1.3 (1) × 10^5 M^{-1} s^{-1},[d] k_w = 0.10 (2) × 10^{-2}/55.5 M^{-1} s^{-1}								
					ROH = CH_2ClCH_2OH (pK = 14.31)[a]								
1	0.010	4.23	0.70 (8)	0.45 (5)	40 (3)	0.4 (1)	4	0.100	4.98	1.3 (1)	0.28 (2)[b]	5 (1)	1.0 (2)
	0.050	3.57	2.5 (3)	2.1 (1)				0.250	4.49	2.09 (6)	0.39 (2)[b]		
	0.100	3.26	4.4 (5)	4.1 (2)				0.500	3.97	2.8 (2)	0.93 (2)[b]		
2	0.010	4.75	0.48 (4)	0.30 (1)	36 (2)	0.10 (5)		0.750	3.47	5 (2)	2.6 (1)[b]		
	0.050	4.00	1.82 (6)	0.79 (2)				0.900	3.01	5 (2)	6.7 (3)[b]		
	0.100	3.70	3.3 (3)	1.50 (5)			5	0.150	5.32	2.59 (3)	0.48 (4)	1.7 (1)	2.4 (2)
	0.250	3.06	9.6 (2)	5.8 (2)				0.350	4.82	2.00 (4)	0.31 (2)		
3	0.010	5.52	0.6 (1)	0.49 (2)	8.4 (8)	0.6 (1)		0.650	4.28	1.82 (5)	0.58 (2)		
	0.100	4.43	1.5 (1)	0.42 (3)[b]				0.900	3.61	1.86 (4)	1.96 (4)		
	0.250	3.95	2.44 (3)	0.96 (1)[b]			6	0.500	6.17	9 (1)	1.7 (1)	1.5 (5)	17 (2)
	0.400	3.61	2.7 (2)	1.4 (1)[b]				0.750	5.65	5.86 (2)	0.67 (2)		
								0.900	4.99	2.66 (2)	0.31 (2)		
					k_H = 70 (4) M^{-1} s^{-1},[c] k_{HO} = 1.7 (1) × 10^6 M^{-1} s^{-1},[d] k_w = 0.10 (2) × 10^{-2}/55.5 M^{-1} s^{-1}								

Table II (Continued)

catal[g]	fraction acid	pH	10^2k_{cat}/ M^{-1} s^{-1}	$10^2k_0/s^{-1}$	10^2k_{HB}/ M^{-1} s^{-1}	10^2k_B/ M^{-1} s^{-1}	catal[g]	fraction acid	pH	10^2k_{cat}/ M^{-1} s^{-1}	$10^2k_0/s^{-1}$	10^2k_{HB}/ M^{-1} s^{-1}	10^2k_B/ M^{-1} s^{-1}
					ROH = $CHCl_2CH_2OH$ (pK = 12.89)[a]								
1	0.010	4.23	0.7 (2)	1.05 (5)	25 (5)	0.4 (2)	4	0.250	4.49	2.3 (3)	1.35 (5)[b]	2.5 (5)	2.5 (5)
	0.050	3.57	1.8 (1)	1.25 (5)				0.500	3.97	3.0 (1)	0.95 (5)[b]		
	0.100	3.26	2.3 (1)	2.65 (5)				0.750	3.47	3.1 (5)	1.80 (5)[b]		
	0.182	2.97	5 (1)	4.8 (1)				0.900	3.01	2.0 (7)	4.4 (1)[b]		
2	0.010	4.75	0.9 (3)	2.3 (1)	13 (2)	0.7 (2)	5	0.350	4.82	4.0 (1)	3.2 (1)	1.40 (5)	5.3 (2)
	0.050	4.00	1.3 (3)	0.85 (5)				0.650	4.28	2.7 (1)	1.2 (1)		
	0.100	3.70	1.7 (2)	1.15 (5)				0.800	3.93	1.7 (2)	0.95 (5)		
	0.250	3.06	4.0 (2)	3.7 (2)				0.900	3.61	1.9 (1)	1.15 (5)		
3	0.100	4.43	1.6 (4)	1.2 (1)[b]	3.3 (5)	1.5 (5)	6	0.900	4.99	7.4 (3)	3.5 (1)	0.8 (2)	64 (5)
	0.250	3.95	1.6 (1)	0.90 (5)[b]				0.9590[e]	4.79	3.1 (2)	2.5 (1)[b]		
	0.400	3.61	2.7 (2)	1.4 (1)[b]				0.9873[e]	4.27	1.5 (2)	1.04 (3)[b]		
	0.600	3.23	2.9 (4)	2.75 (5)[b]				0.9925[e]	4.04	1.2 (2)	0.91 (2)[b]		
	0.750	2.92	2.6 (9)	5.4 (1)[b]									
					k_H = 45 (1) M^{-1} s^{-1},[c] k_{HO} = 3.7 (2) × 10^7 M^{-1} s^{-1},[d] k_w = 0.10 (5) × 10^{-2}/55.5 M^{-1} s^{-1}								
					ROH = CF_3CH_2OH (pK = 12.37)[a]								
1	0.010	4.23		5.2 (2)	8.6 (5)	0.5 (2)	4	0.500	3.97	4 (1)	3.1 (1)[b]	1.9 (5)	5.7 (5)
	0.050	3.57	0.9 (2)	1.9 (1)				0.750	3.47	3.3 (6)	1.8 (1)[b]		
	0.100	3.26	1.4 (1)	1.75 (5)				0.900	3.01	2.1 (8)	2.6 (1)[b]		
	0.182	2.97	1.95 (5)	2.54 (2)			5	0.650	4.28	12.7 (3)	5.5 (1)	0.24 (20)	36 (4)
2	0.050	4.00	3 (1)	3.8 (3)	5 (1)	2.5 (5)		0.800	3.93	4.7 (2)	3.0 (1)		
	0.100	3.70	1.5 (4)	2.4 (1)				0.990	2.59	0.6 (2)	5.5 (5)		
	0.250	3.06	3.2 (2)	2.2 (1)			6	0.9932[e]	4.00	4.5 (5)	3.2 (1)[b]	~0	600 (100)
3	0.250	3.95	1.5 (3)	3.00 (5)[b]	1.3 (7)	2.0 (7)		0.9965[e]	3.71	1.8 (2)	2.1 (1)[b]		
	0.400	3.61	2.16 (8)	1.95 (2)[b]				1.0000		~0[f]			
	0.600	3.23	1.21 (7)	1.95 (2)[b]									
	0.750	2.92	1.5 (2)	2.85 (5)[b]									
					k_H = 20 (1) M^{-1} s^{-1},[c] k_{HO} = 2.7 (2) × 10^8 M^{-1} s^{-1},[d] k_w = 0.35 (15) × 10^{-2}/55.5 M^{-1} s^{-1}								

[a] Reference 25. [b] Interpolation from pH profile. [c] In terms of antilg (−pH). [d] In terms of antilg (pH −14). [e] Calculated from measured pH and the two acidity constants for cacodylic acid ($pK_a(cacH_2^+)$ = 1.77,[39] $pK_a(cacH)$ = 6.16), i.e., the figure includes contributions from both acids. [f] Assumed. [g] The catalysts are: 1. cyanoacetic acid (pK_a = 2.23); 2. chloroacetic acid (pK_a = 2.70); 3. methoxyacetic acid (pK_a = 3.40); 4. 3-chloropropionic acid (pK_a = 3.93); 5. acetic acid (pK_a = 4.65); 6. cacodylic acid (pK_a = 6.16). Acidity constants at I = 1.0 were determined from pH in solutions of known buffer ratio.

The second-order rate constants for the buffer-catalyzed breakdown of acetaldehyde hemiacetals and hydrate are also given in Table II. They were obtained as described in the Experimental Section from plots of k_{obsd} against total buffer concentration for different buffer ratios (Table II), as shown in Figure 3 for the breakdown of acetaldehyde hydrate. The slopes of these plots against percent buffer acid are shown in the inset. The values of k_{HB} and k_B are found as the two intercepts. The extensive studies at 65% acid in Figure 3 show that (1) no third-order term, k_3[HAc][Ac^-], due to true bifunctional catalysis[29,30] and expected to cause upward curvature, is experimentally detectable and (2) trapping with semicarbazide in the concentration range 0.0033–0.0067 M is complete and catalysis by this species is negligible.

Kinetic data for the hydration/dehydration of acetaldehyde are reported in a number of literature sources.[3,27,28a,31] Despite variations in experimental techniques and other conditions, the agreement with our data is satisfactory. In a very recent investigation Chiang and Kresge[31] report the following data for the decomposition of acetaldehyde ethyl hemiacetal in aqueous solution at 25 °C and I = 0.10 M, studied by a trapping technique: k_H = 110 M^{-1} s^{-1} (145); k_w = 1.2 × 10^{-3} s^{-1} (1.5 × 10^{-3}); k_{HAc} = 5.6 × 10^{-2} M^{-1} s^{-1} (6.2 × 10^{-2}); and k_{Ac^-} = 3.6 × 10^{-2} M^{-1} s^{-1} (2.4 × 10^{-2}). These rate constants are in good agreement with ours (given in parentheses) when the difference in ionic strength is taken into account. Thus, even the reciprocal relationship between rate ratios for k_{HAc} and k_{Ac^-}, respectively, may be explained qualitatively by means of activity coefficients.

Useful Equilibrium and Rate Constants. The "spectrum" of potential mechanisms associated with the decomposition of a hemiacetal or hydrate, involving two proton transfers and the breaking of a C–O bond as elementary steps, may be visualized by Figure 4 where acid and base catalysis can be displayed simultaneously. A fully stepwise reaction from R^0 to P^0 in Figure 4 is illustrated by following the edges while coupling between steps appears by passage over the surface or through the interior of the

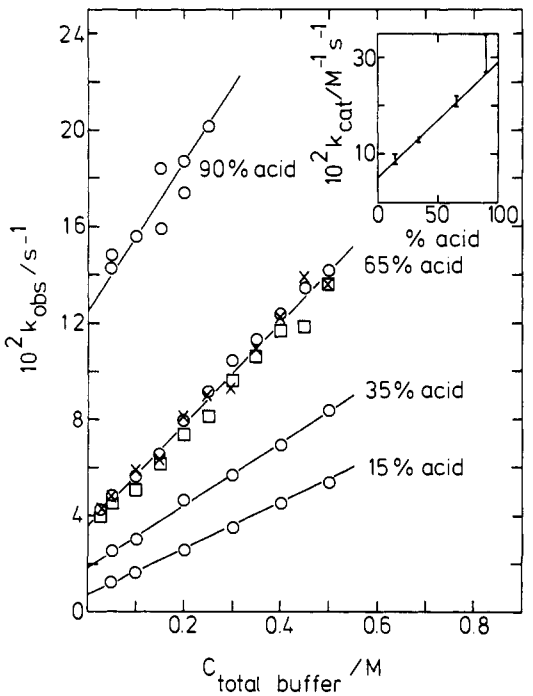

Figure 3. The breakdown of acetaldehyde hydrate catalyzed by acetate buffers of varying buffer ratios. The concentrations of semicarbazide in 65% acidic buffer were 6.67 × 10^{-3} M (X), 5.0 × 10^{-3} M (○), and 3.33 × 10^{-3} M (□). Inset: dependence of the slopes of the lines (k_{cat}) on the buffer composition.

(29) Bell, R. P. *The Proton in Chemistry*, 2nd ed.; Chapman and Hall: London, 1973. Jencks, W. P. *Catalysis in Chemistry and Enzymology*; McGraw-Hill: New York, 1969.
(30) Hegarty, A. F.; Jencks, W. P. *J. Am. Chem. Soc.* **1975**, *97*, 7188.
(31) Chiang, Y.; Kresge, A. J. *J. Org. Chem.* **1985**, *50*, 5038.

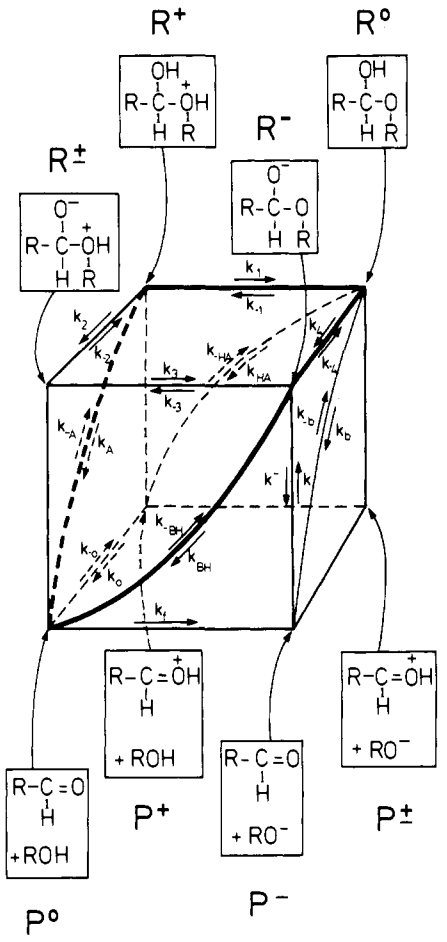

Figure 4. A cube to show possible mechanisms for the addition of ROH to aldehydes with acid and base catalysis. Proton transfer takes place along the horizontal axes and C–O bond formation/breaking takes place along the vertical axes.

cube. The methods for derivation of the various constants in Figure 4 were described in detail by Funderburk et al.[7] and only a brief description is given here. In Table III we present formulae and data derived for acetaldehyde together with those for formaldehyde (in parentheses) for comparison,[7,32] including rate constants for proton-transfer steps.[33,34]

If the acidity constants for the species in Figure 4 are known, or can be estimated, the various rate constants may be derived. These (hypothetical) rate constants may be useful, since in some cases certain mechanisms can be excluded if a calculated rate constant exceeds that for a diffusion-controlled reaction, or if an experimentally observed reaction rate is faster than can be accounted for by a rate-determining step characterized by the calculated rate constant of a particular mechanism.

pK_4. This was calculated from a statistically corrected value of pK_a = 13.87 for acetaldehyde hydrate[35] and from pK_a values of the parent alcohols by using a fall-off factor of 0.2.[7] The decrease in acid strength by a factor of two as a result of substituting an α-hydrogen atom with a methyl group is in good agreement with predictions from the general Taft equation, log $(K/K_0) = \sigma^*\rho^* = (-0.10) \times 3.47 = -0.347$, for acid dissociation of RCH_2OH (H_2O, 25 °C) reported by Wells.[36]

pK_1. The pK_a values for the conjugate acids of acetaldehyde hydrate and trifluoroethyl hemiacetal are obtained by adding 0.3 pK units to the values for the corresponding formaldehyde derivatives in Table III. In the case of protonated acetaldehyde ethyl hemiacetal only 0.2 is added, resulting in a pK_a of −4.4 for this substance, because the difference between experimentally obtained pK_a values of protonated diethyl ether (−2.42) and methyl ethyl ether (−2.60) is 0.18.[37]

pK_2. This is taken as pK_4 − 4.7; the difference of 4.7 pK units originates from the effect of the positive charge on R^+.[7]

pK_3. From the requirement pK_3 = pK_1 + pK_4 − pK_2.

In the *acid-catalyzed breakdown* reaction ($R^0 \rightarrow P^0$ in Figure 4) two mechanisms involving concerted steps should be considered: $R^0 \rightarrow R^+ \rightarrow P^0$ (class e, eq 1) and $R^0 \rightarrow P^+ \rightarrow P^0$ (class n). The rate constant k_{-1}' for protonation by HB of the leaving group of the hemiacetal or hydrate, R^0, in a *class e mechanism* is given in Table III. Here the rate constants for protonation by water and the solvated proton, respectively, represent two extremes. Thus, protonation of acetaldehyde hydrate by water is characterized by $k_{-1}' = 4.0 \times 10^{-8}$ s^{-1}, which is 10^5 times slower than the observed spontaneous rate constant for cleavage (Table II) and excludes this mechanism for the water reaction. On the other hand, the rate constant for protonation of the hydrate by the solvated proton, $k_{-1}' = 2.2 \times 10^8$ M^{-1} s^{-1}, is more than adequate to account for the observed rate. This latter statement is also valid for the acid catalysts in the intermediate pK range, apart from the decomposition of acetaldehyde trifluoroethyl hemiacetal (the weakest base of the addition compounds (Table III)), for which $k_{-1}' = 2.2 \times 10^{-3}$ M^{-1} s^{-1} for catalysis by the weaker acid, acetic acid, is essentially equal to the experimental catalytic constant (Table II).

Further evidence in favor of a class e mechanism based on individual rate constants is given in the Discussion.

In the *class n mechanism* for the acid-catalyzed formation of hydrate or hemiacetal, $R^0 \rightarrow P^+ \rightarrow P^0$ in Figure 4, k_{-HA} has been determined and a selection of values is given in Table III.

The two most plausible pathways in the *base-catalyzed breakdown reaction*, $R^0 \rightarrow P^0$ in Figure 4, are indicated as $R^0 \rightarrow R^- \rightarrow P^0$ (class n, eq 2) and $R^0 \rightarrow P^- \rightarrow P^0$ (class e). Individual rate constants for the various steps can be calculated and are given in Table III.

A possible base-catalyzed decomposition route goes in a stepwise manner from R^0 via R^- and $R^\pm$ to P^0 in Figure 4. Overall rate constants for the formation of $R^\pm$ are given by $k_{-3}'K_4/K_{HB} = k_3'K_4/K_3$, thus independent of K_{HB} (Table III, the prime indicates proton transfer involving a buffer base or acid). Another fully stepwise route of $R^0 \rightarrow R^- \rightarrow P^- \rightarrow P^0$ is unlikely for most bases, since in the reverse reaction the deprotonation of the nucleophile in the step $P^0 \rightarrow P^-$ is too slow to account for the observed rate. Thus, as shown by Funderburk et al.,[7] the second-order rate constant k_f' for the removal of a proton from water by cyanoacetate to form hydroxide ion is equal to 3.1×10^{-4} M^{-1} s^{-1}, 15.5 times smaller than k_{-BH}.

As shown for formaldehyde by Funderburk et al.,[7] the barriers for breakdown of the two intermediates in catalysis of the acetaldehyde reactions by the hydroxide ion, R^- and P^- in Figure 4, are generally sufficiently high to provide these species with significant, though short, lifetimes. Thus, the rate constants k^- for breakdown of R^-, given by $k^- = k_{HO}K_w/K_4$, range from 6.4×10^3 s^{-1} for the hydrate to 3.8×10^7 s^{-1} for the trifluoroethyl hemiacetal. The rate constants for attack of hydroxide and ethoxide ions on formaldehyde, calculated as $k = k_{HO}/K_d$, are 4.8×10^6 and 6.5×10^7 M^{-1} s^{-1}, respectively, which is well below the diffusion-controlled limit, and therefore must give rise to a significant barrier. However, since these rate constants are large both for formaldehyde and acetaldehyde, it is unlikely that there will be a significant barrier for the attack of alkoxide ions on the protonated carbonyl compound (P^+ in Figure 4). Discussions of mechanism involving this pathway are therefore avoided in the present paper.

Funderburk et al.[7] found for formaldehyde that the two intermediates in *acid catalysis*, R^+ and P^+ in Figure 4, have sig-

(32) A few minor errors in the data for formaldehyde[7] have been corrected.
(33) Eigen, M. *Angew. Chem., Int. Ed. Engl.* **1964**, *3*, 1.
(34) Ahrens, M. L.; Maass, G. *Angew. Chem., Int. Ed. Engl.* **1968**, *7*, 818.
(35) Bell, R. P.; Onwood, D. P. *Trans. Faraday Soc.* **1962**, *58*, 1557.
(36) Wells, R. P. *Linear Free Energy Relationships*; Academic Press: London, New York, 1968; p 38.
(37) Bonvinci, P.; Levi, A.; Lucchini, V.; Modena, G.; Scoranno, G. *J. Am. Chem. Soc.* **1973**, *95*, 5960.

Table III. Calculated or Estimated Equilibrium and Rate Constants for Reactions of Acetaldehyde and Formaldehyde Hydrate and Hemiacetals[a,b,g]

constant	constant derived from	$CH_3CH(OH)_2$ ($CH_2(OH)_2$)	$CH_3CH(OH)OEt$ ($CH_2(OH)OEt$)	$CH_3CH(OH)OEtF_3$ ($CH_2(OH)OEtF_3$)
pK_1	see text	−3.4	−4.4	−8.0
		(−3.7)	(−4.6)	(−8.3)
pK_2	see text	9.2	9.2	8.4
		(8.9)	(8.9)	(8.2)
pK_3	see text	1.0	0.4	−3.2
		(0.7)	(0.1)	(−3.6)
pK_4	see text	13.57	13.86	13.14
		(13.27)	(13.56)	(12.85)
$k_2(HOH)^c$	$k_{-2}K_2$[h]	6.3	6.3	40
		(12.6)	(12.6)	(63)
$k_2'(CNAc)^d$	$k_{-2}K_2/K_{HB}$[i]	107	107	676
		(213)	(213)	(1070)
$k_{-3}'K_4/K_{HB}(Ac)^d$	$k_3'K_4/K_3$[j]	2.7×10^{-3}	3.5×10^{-4}	4.6×10^{-7}
		(2.7×10^{-3})	(3.5×10^{-4})	(3.5×10^{-7})
k_4^c	$k_{-4}K_4$[k]	2.7×10^{-4}	1.4×10^{-4}	7.2×10^{-4}
		(5.4×10^{-4})	(2.8×10^{-4})	(1.4×10^{-3})
$k_4'(CNAc)^d$	$k_{-4}K_4/K_{HB}$[l]	4.6×10^{-3}	2.3×10^{-3}	1.2×10^{-2}
		(9.1×10^{-3})	(4.6×10^{-3})	(2.3×10^{-2})
$k_{BH}(CNAc)^d$	k_BK_{HB}/K_4[m]	8.8×10^8	5.1×10^8	4.1×10^8
		(5.5×10^8)	(3.2×10^8)	(4.3×10^7)
$k_{BH}(H^+)^d$		1.8×10^{11}	1.1×10^{11}	4.8×10^{10}
		(7.8×10^{10})	(5.8×10^{10})	(3.0×10^9)
$k_{-BH}(CNAc)$	k_B/K_d[n]	4.8×10^{-3}[d]	5.8×10^{-4}[e]	
		(11)[d]	(1.3)[e]	
$k_{-b}'(CNAc)^e$	$k_{-BH}K_{HB}/K_d$[n]	2.8×10^9	3.5×10^{10}	
		(6.5×10^{12})	(7.7×10^{13})	
$k_{-b}'(H^+)^e$		6.0×10^{11}		
		(9.7×10^{14})		
$k_A(HOH)^c$	$k_{HB}K_1/K_{HB}$[o]	1.4×10^6	3.7×10^6	2.0×10^9
		(1.4×10^4)	(2.9×10^4)	(2.4×10^7)
$k_A(CNAc)^d$		1.7×10^6	4.3×10^6	1.5×10^9
		(9.2×10^4)	(2.0×10^5)	(9.8×10^7)
$k_A(Ac)^d$		3.3×10^7	7.0×10^7	1.1×10^{10}
		(5.1×10^6)	(1.2×10^7)	(3.1×10^9)
$k_A(HO^-)^d$		1.2×10^{15}	3.7×10^{15}	3.5×10^{19}
		(2.1×10^{15})	(6.4×10^{15})	(8.4×10^{18})
$k_{-A}(Ac)$	k_{HB}/K_d[n,o,p]	3.5×10^{-1}[d]	2.7×10^{-2}[e]	2.5×10^{-4}[e]
		(5.1×10^1)[d]	(5.9)[e]	(7.0×10^{-2})[e]
$k_{-A}(CNAc)$		4.7[d]	4.4×10^{-1}[e]	9.1×10^{-3}[e]
		(2.45×10^2)[d]	(2.5×10^1)[e]	(5.8×10^{-1})[e]
$k_{-A}(H^+)$		6.83×10^2[d]	6.4×10^1[e]	2.1[e]
		(6.5×10^3)[d]	(6.2×10^2)[e]	(2.4×10^1)[e]
$k_{-HA}(Ac)$	$k_{-A}K_0/K_{HB}$[q]	9.9×10^7[d]	7.7×10^6[e]	7.2×10^4[e]
		(1.4×10^9)[d]	(1.7×10^8)[e,f]	(2.2×10^6)[e,f]
$k_{-HA}(CNAc)$		5.0×10^6[d]	4.70×10^5[e]	9.8×10^3[e]
		$(2.6 \times 10^7$[d,f]	(2.8×10^6)[e,f]	(6.9×10^4)[e,f]
$k_{-HA}(H^+)$		4.3×10^6[c]	4.1×10^5[d]	1.3×10^4[d]
		(4.1×10^6)[c,f]	(4.2×10^5)[d,f]	1.7×10^4[d,f]
$k_f'(CNAc)^d$	$k_{-f}'K_{ROH}/K_{HB}$[r]	3.1×10^{-4}	1.7×10^{-4}	7.2×10^{-1}
		(3.1×10^{-4})	(1.7×10^{-4})	(7.2×10^{-1})
$k_{-1}(HOH)^d$	$k_1'K_{HB}/K_1$[s]	4.0×10^{-8}	4.0×10^{-9}	1.0×10^{-12}
		(2.0×10^{-8})	(2.0×10^{-9})	(5.0×10^{-13})
$k_{-1}'(H^+)^d$		2.2×10^8	2.2×10^7	5.5×10^3
		(1.1×10^8)	(1.4×10^7)	(2.8×10^3)
$k_{-1}'(Ac)^d$		89	8.9	2.2×10^{-3}
		(45)	(5.6)	(1.1×10^{-3})
$k_{-0}'(CNAc)^d$	$k_0'K_{HB}/K_0$[t,q]	9.3×10^3[u]		
		(9.3×10^4)		
$k_{-0}'(CaC)^d$		1.1[u]		
		(11)		
$k_{-0}'(H^+)$		8.7×10^7[u]		
		(8.7×10^8)		

[a] Values for formaldehyde in parentheses taken from ref 7. [b] The rate and equilibrium constants are defined in Figure 4 and the text. [c] s^{-1}. [d] M^{-1} s^{-1}. [e] M^{-2} s^{-1}. [f] Lower limits, assuming $pK_0 = -2.8$ for protonated formaldehyde. [g] The primed constants refer to catalysis by buffer acids and bases. [h] k_{-2} taken as 10^{10} M^{-1} s^{-1}.[7,33] [i] k_{-2}' taken as 10^{-9} M^{-1} s^{-1}.[7,33] [j] k_3' taken as 10^{10} M^{-1} s^{-1}.[7,34] [k] k_{-4} taken as 10^{10} M^{-1} s^{-1}.[7,33] [l] k_{-4}' taken as 10^{-9} M^{-1} s^{-1}.[7,33] [m] k_B is the experimental catalytic constant from Table II. [n] $K_d = 0.83$ (this work) for acetaldehyde hydrate and $K_d = 2.1$ M at 25 °C[y] for the ethyl hemiacetal derived from the expression K_d(acetaldehyde ethyl hemiacetal) = K_d(formaldehyde ethyl hemiacetal) × K_d(acetaldehyde hydrate)/K_d(formaldehyde hydrate); a value of K_d(formaldehyde ethyl hemiacetal) = 1.1×10^{-3} M was estimated by Funderburk et al.[7] and K_d(formaldehyde hydrate) was taken as 4.4×10^{-4}.[7] [o] k_{HB} is the experimental catalytic constant from Table II. [p] K_d(acetaldehyde trifluoroethyl hemiacetal) = 9.4 M can be estimated from K_d(formaldehyde trifluoroethyl hemiacetal) = 5.0×10^{-3} M[7] by the procedure described above.[n] [q] K_0 is the acidity constant for protonated acetaldehyde. It is taken as $K_0 = 10^{3.8}$ obtained from a value of $K_0 = 10^{2.85}$ for protonated acetone[v] and a correction of −0.9 pK units for substituting a methyl group with hydrogen; this is based on a reported difference of 0.9 in pK_a values of acetophenone and benzaldehyde.[x] [r] k_{-f}' for the reverse reaction is taken as 10^{10} M^{-1} s^{-1} (not shown in Figure 4), K_{ROH} is the acid dissociation constant of the leaving group. [s] k_1' taken as 10^{10} M^{-1} s^{-1}.[7,34] [t] k_0' taken as 10^{10} M^{-1} s^{-1}. [u] These rate constants are independent of leaving group. [v] Levi, A.; Modena, G.; Scorrano, G. *J. Am. Chem. Soc.* **1974**, *96*, 6585. [w] McClelland, R. A.; Reynolds, W. F. *Can. J. Chem.* **1976**, *54*, 718. [x] Arnett, E. M. *Prog. Phys. Org. Chem.* **1963**, *1*, 351. [y] $K_d^{-1} = (2.1)^{-1} = 0.48$ M^{-1} can be compared with experimental values of $K_d^{-1} = 0.85$ M^{-1} (at 20 °C: Bone, R.; Cullis, P.; Wolfenden, R. *J. Am. Chem. Soc.* **1983**, *105*, 1339) and $K_d^{-1} = 0.70$ M^{-1} (at 25 °C: Guthrie, J. P. *J. Am. Chem. Soc.* **1973**, *95*, 6999) for addition of *methanol* to acetaldehyde in aqueous solution.

Table IV. Brønsted α, β, and β_{lg} Values for the General Acid and Base Catalyzed Decomposition of Acetaldehyde Hemiacetals and Hydrate ($ROCHCH_3OH$), Compared with Equivalent Data for Formaldehyde (in Brackets)[7]

R	pK_{ROH}	β	α	p_{xy}^{B} [a]	$p_{xy}'^{HB}$ [b]
CH_3CH_2	16	0.39 [0.26]	0.51 [0.28]	0.040	0.070
H	15.74	0.39 [0.24]	0.50 [0.29]	0.046	0.064
CH_3	15.54	0.48 [0.26]	0.51 [0.27]	0.067	0.073
$CH_3OCH_2CH_2$	14.82	0.48 [0.34]	0.54 [0.33]	0.043	0.064
$ClCH_2CH_2$	14.31	0.50 [0.34]	0.55 [0.33]	0.049	0.067
Cl_2CHCH_2	12.89	0.55 [0.54]	0.56 [0.36]	0.003	0.061
F_3CCH_2	12.43	0.73 [0.58]	0.59 [0.36]	0.046	0.070
				mean 0.042	mean 0.067

catalyst	pK_{HB}	β_{lg}^{B} [c]	β_{lg}^{HB} [e]	$p_{yy}'^{HB}$ [f]
HO^-	15.74	−0.95[d]		
cacodylate	6.16	−0.204	0.39	
acetate	4.65	−0.092 [−0.119]	0.37 [0.32]	0.015
3-Cl propionate	3.93	−0.039 [−0.051]	0.31 [0.26]	0.015
MeO acetate	3.40	0 [0]	0.39 [0.34]	0.015
Cl acetate	2.70	0.051 [0.066]	0.31 [0.26]	0.015
CN acetate	2.23	0.086 [0.111]	0.30 [0.27]	0.009
H_2O	−1.74	0.32 [0.41][d]	0.25 [0.20]	0.015
				mean 0.014

[a] Defined as $p_{xy} = \partial\beta/-\partial\sigma_{norm} = \partial\beta/3.27$ (see text and ref 19). [b] Defined as $p_{xy'} = \partial\alpha/-\partial\sigma_{norm} = \partial\alpha/3.27$ (see text and ref 19). [c] The values are slopes of the lines in Figure 8, they represent "normalized" slopes. [d] Based on extrapolation. [e] Slopes of lines in Figure 12. [f] Defined as $\partial\beta_{lg}^{HB}/-\partial\sigma_{norm} = \partial\beta_{lg}^{HB}/3.27$.

nificant lifetimes. The rate constant $k_A = 1.4 \times 10^6$ s^{-1} (Table III) for the breakdown of R^+ into acetaldehyde and water also indicates a considerable barrier. The protonated aldehydes P^+ decompose to adduct rapidly but probably have significant barriers; lower limits of k_{-HA} are given in Table III.

Discussion

Acid Catalysis. All acid catalysts studied in the present work, including the hydrogen ion, obey the laws of general acid catalysis. The experimental data for acid catalysis (Table II) are presented in Brønsted plots in Figure 5 and the α values are given in Table IV. The plots are simple least-squares lines, including the points for hydrogen ion catalysis but omitting the points for cacodylic acid, which exhibit large positive deviations from the lines. This might possibly represent a bifunctional component to catalysis from an interaction of the basic site on the catalyst with the partial positive charge on the alcohol in the transition state, **1**.[38] Cacodylic acid is much more basic than carboxylic acids (the pK_a of $(CH_3)_2As(OH)_2^+$ is 1.77).[39] Catalysis of the dehydration of 4-nitrobenzaldehyde hydrate by cacodylic acid shows a smaller or negligible positive deviation;[8] however, the smaller value of α for this compound suggests that there is less proton removal and, therefore, a smaller basicity of the catalyst in the transition state.

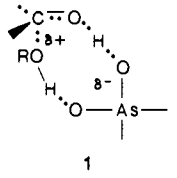

1

Values of β_{lg}, as determined from the slopes of log k_{HB} against pK_{lg} in Figure 6, are all positive and are in the range 0.25–0.39 (Table IV). Literature data for α and β_{lg} obtained for formaldehyde[7] are also given in Table IV (in brackets) for comparison.

General acid catalysis of the reactions of acetaldehyde must proceed through a concerted mechanism because the observed rate constants are too large to be consistent with intermediates along the reaction path that have a significant lifetime. A hydrogen-bonded dipolar intermediate $BH\cdot{}^-OCH_2OHR^+$ was shown to be unlikely but could not be rigorously excluded for addition of the same alcohols to formaldehyde.[7] Stepwise pathways for the acetaldehyde reactions that involve a free intermediate and the hydrogen-bonded intermediate of a preassociation mechanism[7]

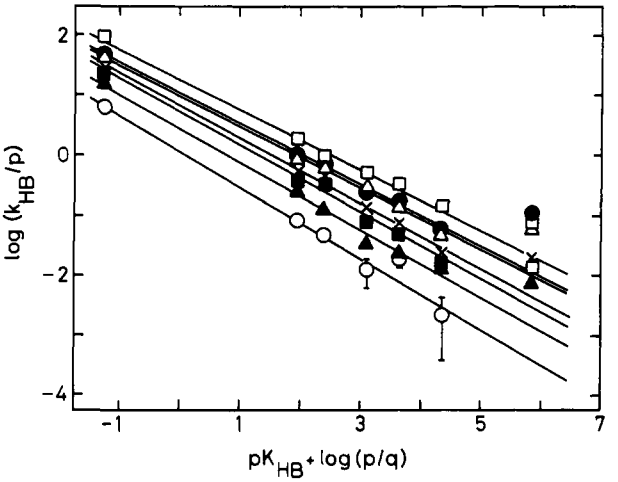

Figure 5. Brønsted plots for general acid catalysis of the cleavage of acetaldehyde hydrate (□), ethyl hemiacetal (●), methyl hemiacetal (△), methoxyethyl hemiacetal (×), chloroethyl hemiacetal (■), dichloroethyl hemiacetal (▲), and trifluoroethyl hemiacetal (○). The lines are least-squares fits to the data, including water but omitting the points for cacodylic acid.

are shown in the lower and upper paths of eq 3, respectively. The lower path is excluded because the rate constant for proton removal, $k_{2'}$, is in general 10^4–10^6 smaller than the observed rate

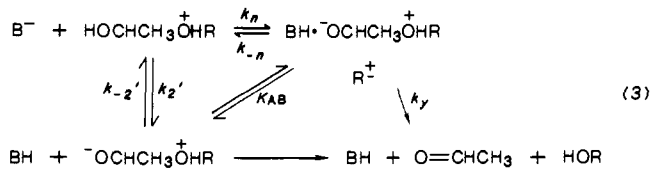

(3)

constant, k_A (Table III). The upper path is excluded because it requires values of $k_{-n} > 10k_y = 10k_{HB}K_1/K_{AB}K_2$ that range from $k_{-n} > 1.8 \times 10^{13}$ s^{-1} for the decomposition of acetaldehyde ethyl hemiacetal catalyzed by cacodylic acid up to $k_{-n} > 1.8 \times 10^{18}$ s^{-1} and $k_y > 1.8 \times 10^{17}$ s^{-1} for decomposition of the trifluoroethyl hemiacetal catalyzed by the solvated proton. A rate constant of $\geq 10^{13}$ s^{-1} is comparable to a vibration frequency so that a chemical species that decomposes with this rate constant cannot exist for several vibrations; i.e., there is no significant barrier for its decomposition and it is not an intermediate. The ratio $k_{-n}/k_y = 10$ was chosen in order for k_y to be rate limiting. Values of the association constant for hydrogen bonding of $K_{AB} = 0.27$ and 2.8

(38) Barnett, R. E.; Jencks, W. P. *J. Am. Chem. Soc.* **1969**, *91*, 2358. Lee, Y. N.; Schmir, G. L. *J. Am. Chem. Soc.* **1979**, *101*, 3026.
(39) Young, P. R.; Jencks, W. P. *J. Am. Chem. Soc.* **1978**, *100*, 1228.

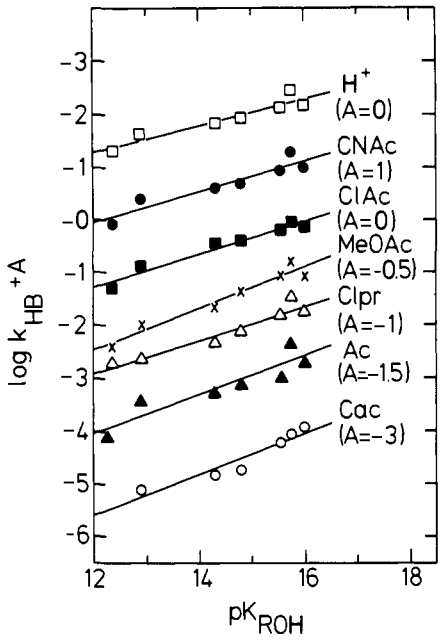

Figure 6. Plots of log k_{HB} against the pK_a of the leaving group for general acid catalysis of the cleavage of acetaldehyde hemiacetals and hydrate. The parameter A is chosen arbitrarily so as to arrange the plots conveniently in the diagram. The catalysts are hydrogen ion (H^+), cyanoacetic acid (CNAc), chloroacetic acid (ClAc), methoxyacetic acid (MeOAc), chloropropionic acid (Clpr), acetic acid (Ac), and cacodylic acid (Cac). The points are from the Brønsted correlations in Figure 5.

M^{-1} for the two reactions were calculated from a modified version of the Hine equation using $\tau = 0.013$ (eq 4).[40]

$$\log K_{AB} = \tau(pK_{AH} - pK_{HOH})(pK_{H_3O^+} - pK_{BH}) - 2.04 \quad (4)$$

A long extrapolation of the known rate constants for breakdown of acetaldehyde hemiacetals suggests the additional conclusion that the dipolar intermediate R$^\pm$ (eq 3) would not have a significant lifetime even if it could be formed. In other words, the concerted reaction mechanism appears to be *enforced* because the intermediate of a stepwise mechanism has no barrier for collapse and cannot exist. Values of k^- for the breakdown of hemiacetal anions (eq 5) were calculated from values of $K = K_4/K_w$ (Table

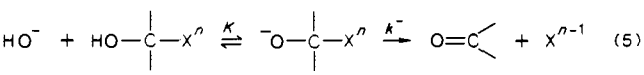

(5)

III), k_{HO} (Table II), and the relationship $k^- = k_{HO}/K$ for the hydrate and the ethyl and trifluoroethyl hemiacetals. A plot of log k^- against pK_{lg} has a slope of $\beta_{lg} = -0.92$ and extrapolation to p$K_a = -1.74$ gives a value of $k^- = 10^{20}$ s^{-1} for the expulsion of water from R$^\pm$. The rate constant for expulsion of trifluoroethanol from the corresponding R$^\pm$ is expected to be some 10^3 faster than this.

These reactions complete the series of mechanisms mentioned in the introduction for acid catalysis of the addition to acetaldehyde of reagents with varying nucleophilicity. The mechanisms in this series are enforced by the lifetime (or the absence of a lifetime) of the intermediate species that would be formed in the absence of catalysis. Thus, no catalysis is observed for the addition of strongly basic thiol anions that form a stable anionic addition intermediate in the rate-limiting step, followed by fast proton transfer from solvent water.[4,41] Addition of the less basic anion of methyl mercaptoacetate gives an addition intermediate that reverts to reactants at a rate comparable to its protonation by water, so that diffusion-controlled protonation by buffer acids traps the intermediate and catalyzes the reaction. Still less basic thiol anions give an intermediate which is so unstable that it undergoes enforced catalysis by a preassociation mechanism with a large rate acceleration from hydrogen bonding in the transition state. The addition of alcohols, which are still weaker nucleophiles, continues this trend and gives a fully concerted preassociation mechanism with $\alpha = 0.50$–0.59. This mechanism appears to be enforced by the nonexistence of the dipolar addition intermediate, R$^\pm$.

However, concerted catalysis can occur in general acid–base catalyzed reactions that involve proton transfer between electronegative atoms even when intermediates for the stepwise reactions have a significant lifetime.[42] This is presumably because the barrier for proton transfer between electronegative atoms is small, so that the advantage from concerted proton transfer is larger than the disadvantage from including an additional process in the transition state. The reactions of acetaldehyde do not appear to be enforced by the nonexistence of the protonated aldehyde, P$^+$, in the presence of ROH. The rate constant for the addition of water to protonated acetaldehyde would be $k_{-HA} \sim 5 \times 10^6$ s^{-1} if the acid-catalyzed reaction proceeded by a class n mechanism through the protonated aldehyde with p$K_0 = -3.8$ (Table III); since it does not proceed by a class n mechanism this is an approximate upper limit.

The addition of amines to substituted benzaldehydes occurs concurrently through two different mechanisms, one of which is stepwise through the dipolar intermediate R$^\pm$ and another involves catalysis by the solvated proton. The proton-catalyzed reaction is probably concerted, which would mean that concerted and stepwise mechanisms of acid catalysis can coexist in this reaction and that concerted catalysis of class e reactions is not always enforced by the nonexistence of R$^\pm$; however, the possibility has not been excluded that the reaction involves catalysis by hydrogen bonding with a very-short-lived intermediate.[43]

Further evidence for a fully concerted mechanism in which proton transfer plays an active role in driving the reaction is provided by estimation of the advantage that can be obtained by simple hydrogen bonding with the catalyst. Such hydrogen bonding cannot account for the observed catalytic constants for acetaldehyde hydration. Ratios of rate constants for catalysis by hydrogen bonding to water and to different acids were calculated from eq 4, which has been shown to describe equilibrium constants for hydrogen bonding in aqueous solution.[40] The ratios were calculated from the observed value of $\tau = 0.013$ and p$K_3 = 9.2$ for the oxygen anion of R$^\pm$ (Table III); hydrogen bonding in the transition state will be weaker than with R$^\pm$ because there is only a partial negative charge on oxygen in the transition state. The calculated values of $k_H/k_{Ac} = 11$ and $k_H/55.5k_w = 4.5$ M^{-1} are much smaller than the observed ratios of 3170 and 1.1×10^5 M^{-1}, respectively. The calculated value of $\alpha = 0.15$ is also much smaller than the observed value of $\alpha = 0.50$. Thus, only a very small fraction of the catalysis can be explained by simple hydrogen bonding and the observed catalysis must be concerted. We conclude that the proton transfer plays an active role in facilitating nucleophilic attack by increasing the electrophilicity of the carbonyl group and trapping the addition compound, not simply a passive role of stabilizing the developing negative charge on oxygen by hydrogen bonding.

The nature of the transition state for the acid-catalyzed reaction may be characterized by structure–reactivity correlations. Changes in these correlations with changing reactant structure, such as "Hammond" or "anti-Hammond" effects, provide a further characterization of the properties of the transition state and can be described by three-dimensional energy contour diagrams.[19,20] They can also be described by energy contour diagrams that are defined by the energies of the reactants and the products of the partial reactions, assuming a diagonal reaction coordinate; it was

(40) Stahl, N.; Jencks, W. P. *J. Am. Chem. Soc.* **1986**, *108*, 4196.
(41) Lienhard, G. E.; Jencks, W. P. *J. Am. Chem. Soc.* **1966**, *88*, 3982.
(42) Palmer, J. L.; Jencks, W. P. *J. Am. Chem. Soc.* **1980**, *102*, 6466. Bernasconi, C. F.; Howard, K. A. *J. Am. Chem. Soc.* **1983**, *105*, 4690. Bernasconi, C. F.; Howard, K. A.; Kanavarioti, A. *J. Am. Chem. Soc.* **1984**, *106*, 6827.
(43) Rosenberg, S.; Silver, S. M.; Sayer, J. M.; Jencks, W. P. *J. Am. Chem. Soc.* **1974**, 96, 7986. Sayer, J. M.; Pinsky, B.; Schonbrunn, A.; Washtien, W. *J. Am. Chem. Soc.* **1974**, *96*, 7998. Jencks, W. P.; Sayer, J. M. *Faraday Symp., Chem. Soc.* **1975**, *10*, 41.

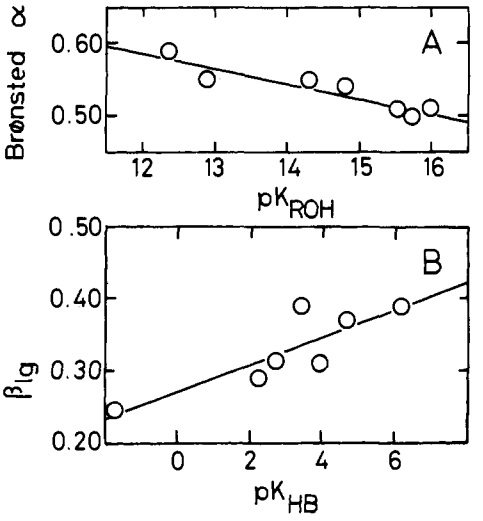

Figure 7. Dependence of the Brønsted coefficient α on pK_{ROH} of the leaving group for general acid catalysis of the cleavage of acetaldehyde hemiacetals and hydrate (A). Dependence of β_{lg}^{BH} on the pK_a of the acid catalysts (B).

concluded from this treatment that the reaction also involves proton transfer between the alcohol and water in the transition state.[44]

As observed for formaldehyde[7] there is a clear tendency for α to increase with decreasing pK of the leaving alcohol or, equivalently, for β_{lg} to increase with decreasing acidity of the catalyzing acid. These changes are described by the cross-correlation parameter $p_{xy} = \partial\alpha/-\partial pK_{lg} = \partial\beta_{lg}/\partial pK_{HB}$.[7,19] Values of $p_{xy} = 0.021$ and $p_{xy} = 0.019$ are found from the plots in Figure 7, A and B, respectively. These data are indistinguishable from a value of $p_{xy} = 0.022$ found for the corresponding formaldehyde reactions.[7] Similarly, p_{xy} was found equal to 0.026 for the acid-catalyzed addition of various thiol anions to acetaldehyde.[4]

A positive value of p_{xy} is an indication of a class e mechanism, i.e., a reaction path corresponding to $R^0 \rightarrow R^+ \rightarrow P^0$ in Figure 4 for hemiacetal cleavage, with the concerted step $R^+ \rightarrow P^0$ being rate-determining. The opposite behavior is expected for a class n mechanism (eq 6).[4,7,19]

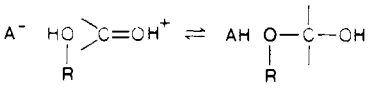

(6)

These structure–reactivity parameters can be described by the energy contour diagram of Figure 8, which is identical with the face $R^+P^+P^0R^\pm$ of the cube in Figure 4. The x and y coordinates of Figure 8 are defined by the observed Brønsted coefficient α for proton transfer in general acid catalysis and β_{lg} for cleavage of the C–O bond in the transition state. Changes in these parameters corresponding to "Hammond" and "anti-Hammond" effects and movement of the transition state parallel and perpendicular to the reaction coordinate, respectively, define the properties of the energy surface around the transition state at the saddle point.[7,18-20]

The approximate (average) positions of the transition states for the formaldehyde and acetaldehyde substrates, as defined by pairs of α and β_{lg}, are indicated in Figure 8 and the reaction coordinates are rotated 45° clockwise from the vertical. This is a reasonable first approximation since curvature in Brønsted plots (Figure 5) or in the plots for determining β_{lg} (Figure 6) has been detected in neither of these two cases ($p_x = p_y = 0$, leading to vertical and horizontal level lines[19]).[45] However, the energy contour lines have been omitted for clarity. The two boxes in Figure 8 indicate the limits for α and β_{lg} given by the experimental data.

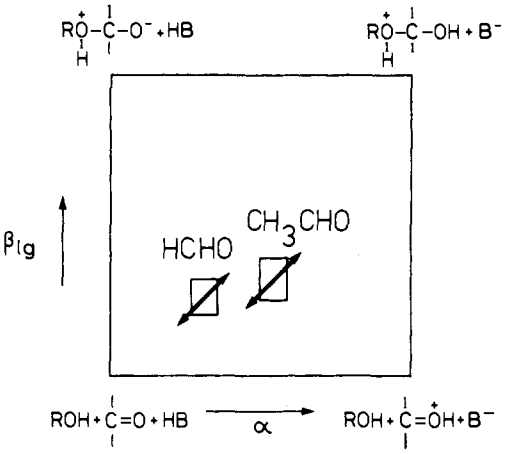

Figure 8. Reaction coordinate-energy contour diagram for general acid catalysis of the reaction of alcohols and water with aldehydes (class e mechanism). The diagram is identical with the face $R^+P^+P^0R^\pm$ of the cube in Figure 4. The x and y axes represent proton transfer and C–O bond formation/breaking as measured by α and β_{lg}^{BH}, respectively (Table IV). The boxes indicate the areas to which the transition states are confined by the experimental values of α and β_{lg}^{BH}.

Since extensive sets of experimental data are now available for the acid-catalyzed decomposition of the hemiacetals and hydrates of both formaldehyde[7] and acetaldehyde, thus reflecting effects of substitution in the electrophile, it is also possible to obtain estimates of the two interaction parameters $p_{xy'} = \partial\alpha/-\partial\sigma_{norm}$ and $p_{yy'} = \partial\beta_{lg}/-\partial\sigma_{norm}$ for a class e mechanism.[19] The "normalized" quantity $\partial\sigma_{norm}$ is taken as −3.27 and the resulting parameters are presented in Table IV. The normalized $\partial\sigma$ value for substituting one hydrogen with methyl in formaldehyde (energy scale based on base 10 logarithms) is obtained as $\partial\sigma_{norm} = \partial\sigma\rho_{eq} = \partial \log K = -3.27$, since $\partial \log K/\partial\sigma = \rho_{eq}$;[19] $\partial \log K$ is taken as $\partial \log K_h$ and K_h(acetald) = 1.22 and K_h(formald) = 2.27×10^3. However, y' parameters for a class e mechanism are not described accurately by a diagonal coordinate on a square diagram because the substitution of methyl for the hydrogen of formaldehyde stabilizes the lower left as well as the lower right corner of Figure 8. Thus, the y' parameter has a significant vertical as well as a diagonal component.

The positive value of $p_{xy'} = 0.067$ is another indication of a class e mechanism.[7,8] Thus, introduction of a CH_3 group for hydrogen in formaldehyde stabilizes the protonated carbonyl group in the lower right corner and, to a smaller extent, the carbonyl group in the lower left corner. This results in movement of the transition state toward the lower right corner, perpendicular to the reaction coordinate (an anti-Hammond effect), and movement toward the upper right corner, parallel to the reaction coordinate (a Hammond effect). The resulting movement to the right corresponds to larger α values for acetaldehyde compared with formaldehyde, as observed. Examples of class n mechanisms in acid catalysis are known, but they give rise to smaller α values as less electronegative substituents are introduced in the electrophile.[46] Our value of $p_{xy'} = 0.067$ is seen to be independent of the leaving group within experimental error (Table IV) and it is very close to a value of $p_{xy'} = 0.070$ calculated from the data by McClelland and Coe for the hydration of a series of benzaldehydes.[8,47]

The small but consistent increase in β_{lg} for acetaldehyde compared with formaldehyde hemiacetals corresponds to a small positive value of $p_{yy'} = \delta\beta_{lg}/-\delta\sigma_{norm} = 0.014$ (Table IV). This means that movement toward the top of the diagram (the Hammond effect) is slightly more important than that toward the bottom (the anti-Hammond effect) when methyl is substituted for the hydrogen of formaldehyde. A positive $p_{yy'}$ coefficient corresponds to an important vertical component to the reaction

(44) Grunwald, E. *J. Am. Chem. Soc.* **1985**, *107*, 4715.
(45) A Hammond effect (positive p_y) was found for the addition of thiol anions to acetaldehyde, i.e., β_{lg} decreases as the nucleophile becomes more basic. This suggests a reaction coordinate with a large vertical component.[4]
(46) See ref 15 and other examples mentioned therein.
(47) The value of $\partial\alpha/\partial\sigma = -0.12$ obtained by McClelland and Coe[8] is converted ("normalized") to an energy scale based on base 10 logarithms by multiplication with ρ_{eq}^{-1} using a value of $\rho_{eq} = 1.71$.[8]

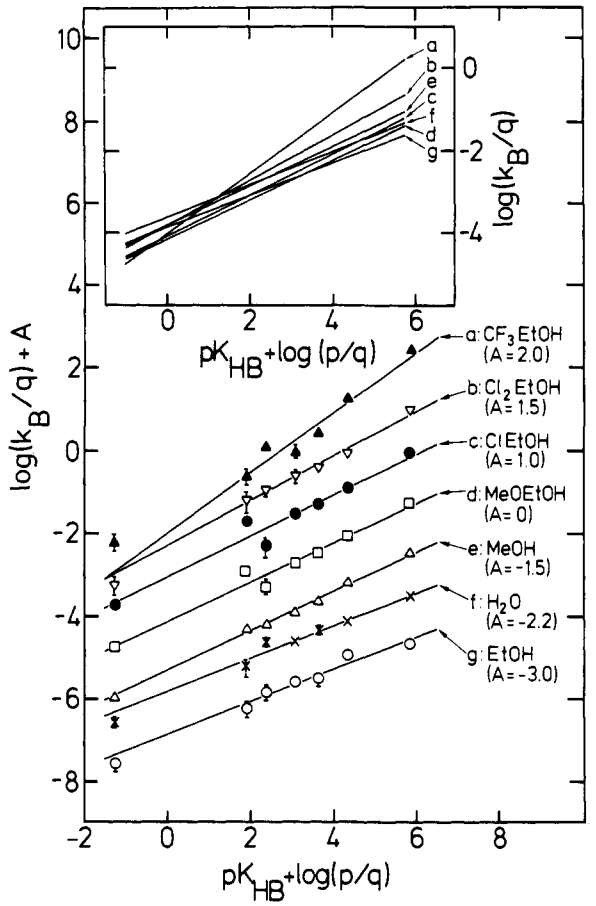

Figure 9. Brønsted plots for general base catalysis of the decomposition of acetaldehyde ethyl hemiacetal (○), hydrate (×), methyl hemiacetal (△), methoxyethyl hemiacetal (□), chloroethyl hemiacetal (●), dichloroethyl hemiacetal (▽), and trifluoroethyl hemiacetal (▲). The rate constants for dehydration have been divided by an additional statistical factor of 2. The parameter A is chosen arbitrarily so as to arrange the plots conveniently; observed positions are shown in the inset. The lines are least-squares fits to the data, omitting the points for water catalysis.

coordinate which, in this case, is accentuated by stabilization of the free as well as the protonated carbonyl group by the CH_3 substituent.

The structure–reactivity data are consistent with a concerted reaction mechanism and a transition state on a diagonal reaction coordinate with an important vertical component in Figure 8. A reaction coordinate rotated 33 ± 13° clockwise from the vertical was calculated for the corresponding formaldehyde reactions[7] and the same limits describe the acetaldehyde reactions, which show very similar interaction coefficients.

We have not attempted to use the $p_{xy'}$ or $p_{yy'}$ coefficients to calculate a reaction coordinate because of the complex nature of the y' coordinate, but the behavior of these coefficients is qualitatively consistent with the same reaction coordinate, with important diagonal and vertical components. The y' coordinate also shows evidence for imbalance in the expression of structure–reactivity behavior in different components of the transition state, as is also observed in the base-catalyzed reactions.[18] The difference of $\sim 10^1$ in the rate constants for the acetaldehyde and formaldehyde hemiacetals is only about 0.3 of the difference of $10^{3.27}$ in the equilibrium constants, suggesting an early transition state for C–O cleavage, while the values of $\beta_{lg} = 0.25$–0.39 suggest 0.6–0.7 cleavage. Possible explanations for this imbalance include incomplete protonation of the leaving alcohol by the solvated proton[44] or a lag in the development of resonance stabilization by hyperconjugation from the CH_3 group in the transition state.[48-50]

(48) Bordwell, F. G.; Boyle, W. J., Jr. *J. Am. Chem. Soc.* **1972**, *94*, 3907.

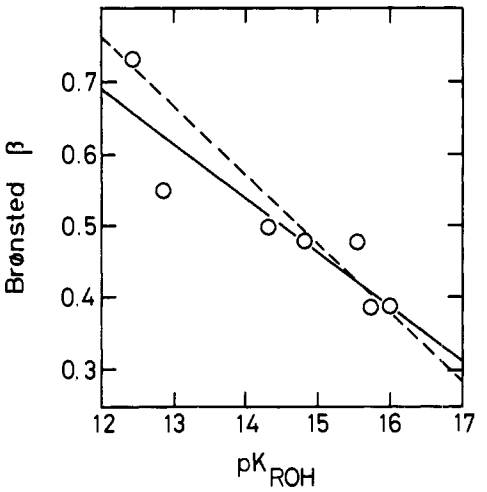

Figure 10. Dependence of the Brønsted coefficient β on the pK of the leaving group for general base catalysis of the cleavage of acetaldehyde hemiacetals and hydrate.

Additional evidence that supports the class e mechanism for acid catalysis of the addition and elimination of ROH, rather than the kinetically equivalent class n mechanism, was described previously.[7] Acid catalysis by a class n mechanism has been observed for addition reactions when the protonated electrophile is more stable, as in the addition of ROH to amidines[15] or imines.[51]

General Base Catalysis. Brønsted plots for general base catalysis of the decomposition reactions, including the "water" reaction, are presented in Figure 9. For the sake of clarity overlapping of the plots is prevented by adjusting the parameter A. The inset shows the correct relative positions, i.e., crossing lines as also observed for formaldehyde.[7] Brønsted β values from the least-squares, linear plots, excluding the points for water catalysis, are given in Table IV where the corresponding figures for formaldehyde[7] are also shown (in brackets) for comparison. Since, in general, the kinetics for acetaldehyde lead to more uncertain data compared with formaldehyde, the points for catalysis by cacodylate anion appear to be useful here. However, due to the extreme value of k_B(cacodylate) = 6 M^{-1} s^{-1} for the cleavage of acetaldehyde trifluoroethyl hemiacetal, this rate constant is difficult to determine experimentally by our technique and a weighting of only 50% has been assigned to this point in calculating β.

It is obvious from Figure 9 that the observed Brønsted β values vary with the leaving group. This represents a cross correlation with a coefficient of $p_{xy'} = \partial\beta/-\partial pK_{lg} = \partial\beta_{lg}/-\partial pK_{BH} = 0.074$, obtained by plotting β against pK_{lg} (Figure 10, solid line).[19] This value is smaller than the value of $p_{xy'} = 0.09$ found for formaldehyde,[7] but it is not certain that the difference is significant because omission of the point for dichloroethanol as leaving group gives a slope of $p_{xy'} = 0.094$ (broken line, Figure 10).

Plots of log k_B against the pK_a of the leaving alcohol in Figure 11 show scatter of the individual points but generally show upward curvature and positive deviations of the rate constants for water and methanol, as observed previously for the corresponding formaldehyde reactions.[7] This curvature shows that the slope, β_{lg}, increases with increasing pK_a of the leaving group; it is described by a negative value of the direct interaction coefficient $p_{y'} = \partial\beta_{lg}/-\partial pK_{lg}$.[19] Again, the lines are separated by an arbitary parameter, A, for clarity.

Values of k_B that are normalized to the rate constants for catalysis by methoxyacetate, log (k_B/k_B(MeOAc)), give lines in plots against pK_{lg} that tend to increase in slope as the pK_a of the catalyst decreases, as shown in Figure 12. This increase in β_{lg} (Table IV) corresponds to the other expression of the $p_{xy'}$ coef-

(49) Kresge, A. J. *Can. J. Chem.* **1974**, *52*, 1897. Bernasconi, C. F. *Tetrahedron* **1985**, *41*, 3219.
(50) Richard, J. P.; Jencks, W. P. *J. Am. Chem. Soc.* **1984**, *106*, 1361.
(51) Sayer, J. M.; Jencks, W. P. *J. Am. Chem. Soc.* **1977**, *99*, 464.

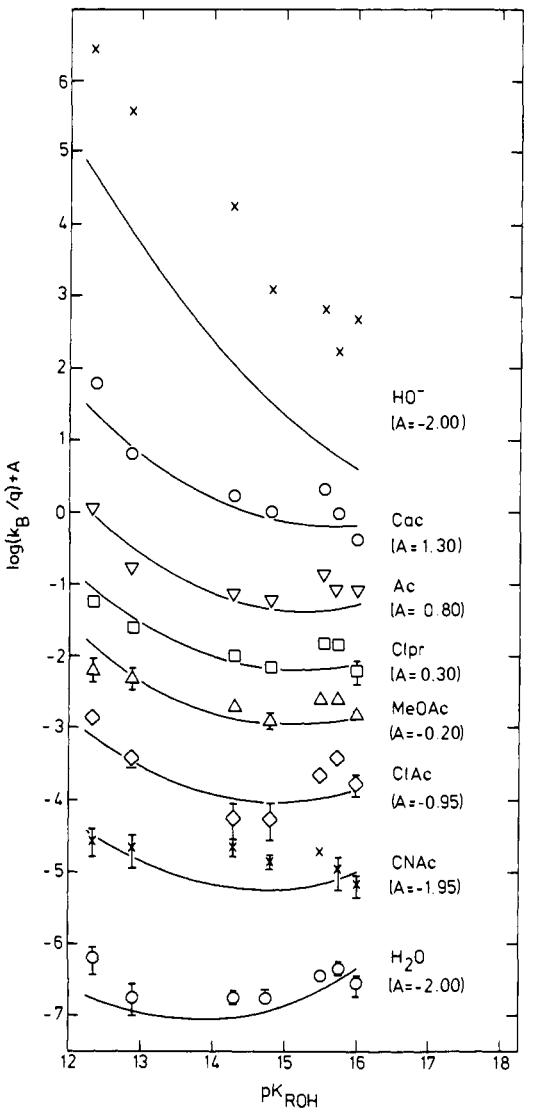

Figure 11. Plots of log k_B against the pK of the leaving group for the base-catalyzed cleavage of acetaldehyde hemiacetals and hydrate. The parameter β_{lg} is obtained from the slopes of the curves which are based on eq 7. The parameter A is chosen arbitrarily and the catalysts are indicated as in Figure 6.

ficient, with a value of $p_{xy} = \partial\beta_{lg}/-\partial pK_{BH} = 0.076$. The absence of significant curvature in these lines means that there is no measurable change in the p_y coefficient with changing pK_a of the catalyst.

The observed rate constants may be described by eq 7, in which $p_x = \partial\beta/-\partial pK_{BH}$ and F is a constant that is taken to fit the absolute values of the rate constants.[7,19] The curves in Figures 11 and 12 are based on eq 7 with the following parameters: $p_x = 0$ (0), p_y

$$-\log k_B = 1/2p_xpK^2_{BH} + 1/2p_ypK^2_{lg} + p_{xy}pK_{BH}pK_{lg} - \beta_0pK_{BH} - \beta^0_{lg}pK_{lg} + F \quad (7)$$

$= -0.20$ (−0.20), $p_{xy} = 0.07$ (0.09), $\beta_0 = 1.53$ (1.68), $\beta^0_{lg} = -2.83$ (−2.58), and $F = -12.92$ (−12.32).[52] The figures in parentheses are for formaldehyde,[7] and it should be noted that p_x as well as p_y is taken to be indistinguishable for the two systems. Although the dependence of log k_B on pK_{lg}, i.e., β_{lg}, changes with pK_{lg} (Figure 11) it is possible to determine this parameter from the slopes of tangents at any given value of pK_{lg} and pK_{BH} by differentiation of eq 7. Thus, we obtain $\beta_{lg} = 0.20pK_{lg} - 0.07pK_{BH} - 2.83$ for acetaldehyde and $\beta_{lg} = 0.20pK_{lg} - 0.09pK_{BH} - 2.58$ for formaldehyde.

(52) The value of $F = -12.075$ in ref 7 should be $F = -12.075 - \log 2 = -12.375$. We have applied $F = -12.32$ in our calculations due to rounded-off values of β_0 and β^0_{lg}.

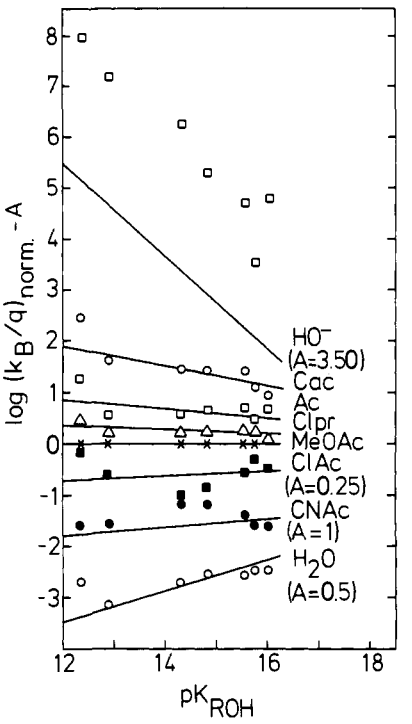

Figure 12. Normalized plots of log k_B against the pK of the leaving group for the base-catalyzed cleavage of acetaldehyde hemiacetals and hydrate. The rate constants are normalized with respect to those for catalysis by methoxyacetate. The parameter A is chosen arbitrarily. The slopes of the lines are given in Table IV. The lines for hydroxide ion and water as catalysts are based on extrapolation from the lines for catalysis by buffer bases.

This overall structure–reactivity picture for the base-catalyzed decomposition of acetaldehyde hemiacetals and hydrate is very similar to that observed for the corresponding formaldehyde derivatives.[7] Hence, there seems to be little doubt that the mechanisms are also the same, i.e., class n as shown in eq 8 and the path $R^0 \rightarrow R^- \rightarrow P^0$ in Figure 4. There is a rapid equilibrium

$$\text{HOCHR'OR} \overset{K_a}{\rightleftharpoons} {}^-\text{O–CHR'–OR} \underset{k_{-BH}[B]}{\overset{k_{BH}[BH]}{\rightleftharpoons}} \text{O=CHR'} + \text{HOR'} \quad (8)$$

dissociation of the hemiacetal hydroxyl proton, followed by concerted leaving group expulsion coupled to partial proton donation to this group in the transition state. The second, rate-limiting step can be illustrated by the reaction coordinate–energy contour diagram in Figure 13A, which corresponds to the face $R^-P^-P^0R^{\pm}$ of the cube in Figure 4.

The coordinates of Figure 13A are defined by the observed structure–reactivity parameters β (which varies from 0 to +1), ρ_{norm} (a normalized ρ value that describes the difference in the reactivity of formaldehyde and acetaldehyde), and β_{lg} (which varies from −1 to +1, from the lower right to the upper left corner of the diagram). The coordinates of the transition state may be defined by two of these parameters. Changes in pK_{BH}, pK_{lg}, or σ_{norm} change the energy of an edge or corners of the diagram and cause a linear perturbation of the energy across the diagram that can produce changes in the energy and position of the saddle point. The amount of the change in position depends on the curvatures around the saddle point and the direction of the reaction coordinate.

Figure 13A shows the positions of the saddle points defined by β and β_{lg} for the decomposition of methoxyethyl hemiacetals of acetaldehyde (A) and formaldehyde (B) catalyzed by methoxyacetate anion. The contour lines are not shown, but the dashed lines show the positions of "level lines" of constant energy that pass through the saddle points. Reaction coordinates are shown that bisect the level lines. The level lines were calculated as described previously[7,19] and correspond to reaction coordinates that are rotated clockwise from the vertical by 48° for form-

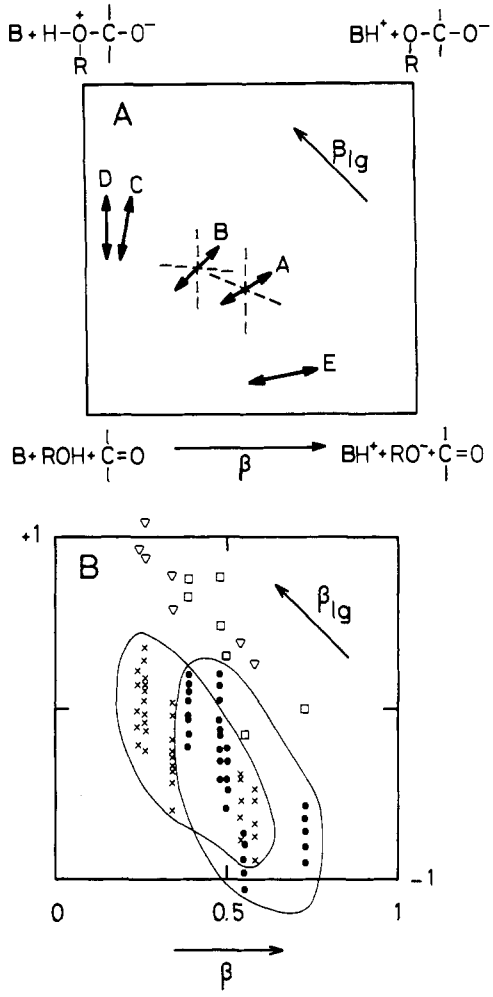

Figure 13. Reaction coordinate–energy contour diagrams for the general base catalyzed reactions of alcohols and water with acetaldehyde (class n mechanism). The diagram is identical with the face $R^-P^-P^0R^\pm$ of the cube in Figure 4. The x and y axes represent proton transfer and C–O bond formation/breaking as measured by β and ρ, respectively. A diagonal axis y' represents charge development on the central oxygen atom, as measured by β_{lg}. (A) The reaction coordinates $A - E$ are discussed in the text; the energy contour lines are omitted. Level lines of constant energy through a saddle point are shown as dashed lines. The reaction coordinate bisects the angle between these lines. (B) Transition-state locations as defined by Brønsted β and β_{lg} values; β_{lg} was calculated by differentiation of eq 7. Notations: hemiacetals, (×), water (▽) (formaldehyde); hemiacetals, (●), water (□) (acetaldehyde).

aldehyde and 57° for acetaldehyde. The difference arises from the difference in $p_{xy'}$ coefficients and is not beyond experimental uncertainty.

Both reaction coordinates are close to diagonal and are consistent with a concerted mechanism in which there is both heavy atom motion and proton transfer in the transition state. If the difference in direction of the reaction coordinates is real it may represent part of a sequence of changes in transition-state properties from the vertical reaction coordinate of specific acid catalysis (D), to a slightly diagonal reaction coordinate for catalysis of addition to unstable carbocations by hydrogen bonding (C), to fully concerted catalysis (B and A), to a largely horizontal reaction coordinate involving primarily proton transfer (E).[12,16,53]

Figure 13B shows the range of movement of the transition states for decomposition of formaldehyde (×) and acetaldehyde (●) hemiacetals as defined by β and β_{lg}. The tendency for movement toward the lower right corner for the less stable acetaldehyde derivatives is evident.

The characteristic features of a class n mechanism are observed in Figure 13:

(1) If changes in catalyst basic strength are considered, a stronger base results in raising the energy of the left-hand side of the diagram compared to the right-hand side. For an almost diagonal reaction coordinate, as observed here, this will result in an overall shift of the transition state toward the bottom of the diagram as the resultant of movements toward the lower right corner, perpendicular to the reaction coordinate, and toward the lower left corner, parallel to the reaction coordinate. This is equivalent to a decrease in β_{lg} and a constant β (linear Brønsted plots), as observed experimentally (it is shown by the vertical sets of points with the stronger bases at the bottom of each set in Figure 13B).

(2) Introducing a more electronegative substituent in the leaving alcohol leads to a lowering of the energy at the lower right corner, whereas the energy is raised at the upper left corner. Such changes cause a principal tendency for the transition state to move the lower right corner as the result of a large (perpendicular) component toward this corner. Such behavior is observed experimentally, since each of the encircled (stretched) areas in Figure 13B comprises points that approach the lower right corner as a result of electron-withdrawing substituents in the alcohol.

(3) Substitution in the third participating molecule in the transition state, the electrophile, is also expected to result in changes of transition-state locations in Figure 13. Thus, replacing one hydrogen by methyl in formaldehyde stabilizes the aldehyde compared to the addition compound. This is manifested by lowering the energy at the bottom of Figure 13 relative to the top. A transition state on an almost diagonal reaction coordinate will now be shifted downhill, perpendicular to the reaction coordinate toward the lower right corner, and also uphill, parallel to the reaction coordinate toward the upper right corner. The resultant of these movements is a shift to the right on the transition-state diagram with an increase in β (cf. the relative positions of transition states in Figure 13A and the encircled areas in Figure 13B.)

The cross-correlation for substitution in the electrophile and nucleophile in a class n mechanism is characterized by the coefficient $p_{yy'} = \partial\beta_{lg}/-\partial\sigma_{norm} = \partial\rho_{norm}/-\partial pK_{lg}$. We have determined $\partial\beta_{lg}$ by plotting log $(k_B(\text{acetald})/k_B(\text{formald}))$ against pK_{lg} for each catalyst. Such plots (Figure 14) show that there is a tendency for this rate constant ratio to decrease with increasing pK_{lg} for all catalysts, except hydroxide ion. The data are consistent with slopes that correspond to $\partial\beta_{lg} = -0.17$ for the two aldehydes, within experimental error. The value of $\partial\sigma_{norm}$ for acetaldehyde and formaldehyde is −3.27, as described above, which gives $p_{yy'} = \partial\beta_{lg}/-\partial\sigma_{norm} = -0.052$. This agrees surprisingly well with the value of $p_{yy'} = -0.048$ that was determined from the secondary α-deuterium isotope effects for catalysis by acetate ion of the cleavage of formaldehyde hemiacetals.[18] The absence of a negative slope for hydroxide ion in Figure 14 is consistent with a different mechanism, specific base catalysis, for this catalyst.

The negative $p_{yy'}$ coefficient is of particular importance because it requires a large horizontal component, corresponding to proton transfer, for the reaction coordinate A in the energy contour diagram of Figure 13A. This is consistent with an active role for proton transfer in the transition state, rather than a passive role of stabilizing the developing charge by hydrogen bonding. It supports the view that this class of reaction should be considered as an electrophilic displacement on the oxygen atom of the alcohol, by an acid in the cleavage direction, and by the electrophilic carbonyl group in the addition direction.[18] When the nature of the transition state changes with decreasing stability of the electrophile, as in general base catalysis of the attack of ROH on 1-phenylethyl carbocations, the reaction coordinate becomes more vertical as shown by C in Figure 13. This corresponds to hydrogen bonding to the catalyst in the transition state, which stabilizes the partial positive charge on ROH. It is manifested experimentally by a positive value of $p_{yy'}$.[16]

(53) Pedersen, K. J.; Pedersen, P. R.; Sørensen, P. E.; Kanagasabapathy, V. M.; McClelland, R. A., in preparation. The base-catalyzed decomposition of some very unstable hemiketals of α-bromoacetophenone shows large Brønsted β values and may therefore be represented by reaction coordinate E in Figure 13A. Preliminary results were presented at the Fourth International Conference on Mechanisms of Reactions in Solution, Canterbury, England, July 7–11, 1986 (R.A.M.).

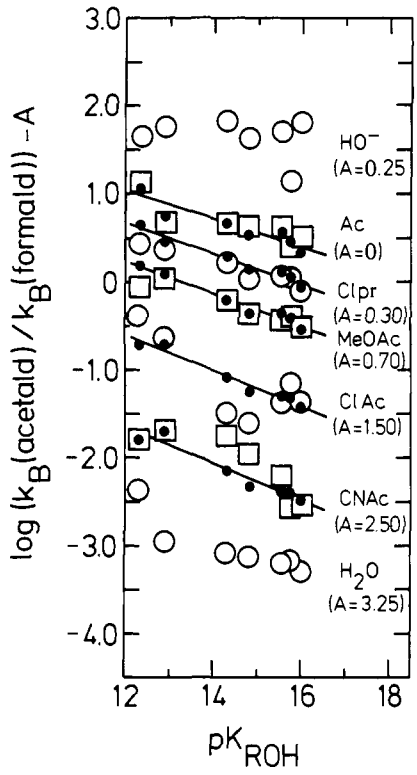

Figure 14. Plots of log k_B against the pK of the leaving group (Table II) for the base-catalyzed cleavage of acetaldehyde hemiacetals and hydrate relative to the corresponding data for formaldehyde.[7] The parameter A is chosen arbitrarily. Open squares and circles are based directly on experimental rate constants. The less scattered small closed circles are ratios of rate constants read from the respective Brønsted plots for the two aldehydes (Figure 9). The lines are least-squares fits to the small closed circles and have slopes in the range -0.17 ± 0.02. The catalysts are indicated as in Figure 6.

Since acetaldehyde is more stable than formaldehyde, we might expect an earlier transition state for hemiacetal cleavage and a later transition state for nucleophilic attack of the alcohol in the reverse direction. This corresponds to a normal "Hammond effect", more positive values of β_{nuc} and β_{lg}, and a positive $p_{xy'}$ coefficient. Instead, the values of β_{nuc} and β_{lg} become more negative because there is more proton removal by the catalyst in order to drive the more difficult reaction in the addition direction; there is less proton addition in the more facile cleavage reaction. This is true even for the water reaction. The second term of the $p_{xy'}$ coefficient, $\partial\rho/-\partial pK_{nuc}$, predicts *less* bond formation when the nucleophile is weaker for a negative value of $p_{xy'}$. This is observed for reactions of alcohols with formaldehyde, as measured by secondary deuterium isotope effects.[18] All of this is consistent with a major, active role of proton transfer in driving the reaction. The negative $p_{y'}$ coefficient, from the upward curvature of the plots of log k against pK_{lg} in Figure 11, is a closely related expression of this behavior. It corresponds to an energy well for the alcohol oxygen atom, between the upper left and lower right corners of the diagram and perpendicular to the diagonal reaction coordinate.[18] This curvature also disappears with more reactive electrophiles, corresponding to reaction coordinate C in Figure 13.[16]

The increase in β for acetaldehyde, a more stable electrophile than formaldehyde, corresponds to a normalized positive coefficient $p_{xy} = \partial\beta/-\partial\sigma = \partial\rho/-\partial pK_{BH} = 0.042$ (Table IV). This is the behavior that is expected for a concerted class n mechanism with a largely diagonal reaction coordinate;[7,8,19] the opposite behavior is observed for catalysis by a class e mechanism (eq 9), as described above for the general acid catalyzed reaction. This value is similar to a normalized value of $p_{xy} = 0.035$ for benzaldehyde hydration[8]

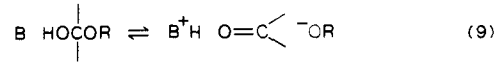

(9)

and a crude value of $p_{xy} = 0.027$ for corresponding reactions of formaldehyde that was estimated from secondary deuterium isotope effects.[18] It is smaller than a normalized value of $p_{xy} = 0.06$ for the acid-catalyzed cleavage of substituted benzaldehyde methyl phenyl acetals[12] and larger than $p_{xy} = 0.014$ for acid-catalyzed cleavage of Meisenheimer complexes[13] and $p_{xy} = 0.014$ for base catalysis of the addition of alcohols to substituted 1-phenylethyl carbocations.[12] The small value for the latter reaction may reflect a large vertical component in the reaction coordinate, as shown in C of Figure 13A.

This change in interaction coefficient and in the direction of the reaction coordinate represents a change in the *nature* of the transition state and reaction mechanism. In the limit, the value of β becomes 0, α becomes 1.0, and the reaction proceeds by specific acid catalysis,[54] as shown in D of Figure 13. These changes occur as β becomes small (or α becomes large) when the electrophile becomes reactive, ROH becomes more basic, and the reaction coordinate approaches the left edge of the diagram. They may be described by interaction coefficients such as $p^*_{xyy'} = \partial p_{xy}/-\partial pK_{nuc} = \partial p_{xy'}/-\partial\sigma = \partial p_{yy'}/-\partial pK_{BH}$, which are third derivatives of log k.[12] A change toward the largely horizontal reaction coordinate, E in Figure 13, might be expected with increasing β and increasing stability of the electrophile and acidity of ROH, but it has not yet been observed. Such a mechanism may be difficult to detect because of competition from specific base catalysis (or the reaction of RO^-), which becomes relatively fast for acidic ROH molecules.

The value of $p_{xy'} = 0.07$ is considerably larger than $p_{xy} = 0.035$; similar differences are found between $p_{xy'} = 0.09$ and $p_{xy} = 0.035$ for formaldehyde hemiacetals[18] and the values of $p_{xy'}$ and p_{xy} for the dehydration of carbinolamines.[55,56] These coefficients are related by eq 10 if all of the structure–reactivity coefficients can be described by a single diagram and are balanced; failure of eq 10 means that there are more changes in the structure of the

$$p_{xy} = p_{xy'} + p_x \qquad (10)$$

transition states than are described by a single diagram for these complex reactions.[18] The linear Brønsted plots for most of these reactions correspond to $p_x = \partial\beta/-\partial pK_{BH} \sim 0$ and suggest that there is imbalance. A small fraction of the difference can be accounted for by an electrostatic interaction between substituents on ROH and HA,[19,57] and it is possible that the linear Brønsted plots conceal upward curvature in both the catalytic constants and the reference ionization reaction;[40] furthermore, upward curvature has been observed in an extended Brønsted plot based on different classes of catalysts for the mutarotation of glucose.[58] However, it is unlikely that these contributions can account for the large differences between p_{xy} and $p_{xy'}$, which have been attributed to an overall loosening of the transition state as ROH becomes less basic.[18,55]

The absolute values of the rate constants for concerted and stepwise reaction pathways support the conclusion that the concerted reaction pathway is followed in order to avoid the formation of the extremely unstable dipolar intermediate, $R^{\pm}$. The extrapolation described in the previous section suggests that the $R^{\pm}$ intermediate is too unstable to have a significant lifetime, so that the concerted mechanism is enforced by the nonexistence of the intermediate that would be required for a stepwise mechanism. However, other class n reactions proceed by a concerted mechanism when the intermediate does exist, so that they are not enforced.[42] As in the case of the acid-catalyzed reaction, the intermediate for the stepwise bimolecular addition reaction in the lower right corner has a significant lifetime; in fact, it is an intermediate in the specific base catalyzed pathway that occurs

(54) Cordes, E. H.; Bull, H. G. *Chem. Rev.* **1974**, *74*, 581.
(55) Funderburk, L. H.; Jencks, W. P. *J. Am. Chem. Soc.* **1978**, *100*, 6708.
(56) There is also a large difference between $p_{xy'} = 0.12$ and $p_{xy} = 0.014$ for the acid-catalyzed decomposition of Meisenheimer complexes;[13] however, this reaction is complicated by the fact that the remaining alcohol as well as the leaving alcohol is changed when ROH is varied.
(57) Rothenberg, M. E.; Richard, J. P.; Jencks, W. P. *J. Am. Chem. Soc.* **1985**, *107*, 1340.
(58) Nielsen, H.; Sørensen, P. E. *Acta Chem. Scand.* **1984**, *A38*, 309.

concurrently with general base catalysis.

The overall rate constant for rate-limiting protonation by acetic acid of the ether oxygen atom of acetaldehyde trifluoroethyl hemiacetal anion to give $R^{\pm}$ in the acetate-catalyzed reaction is $k_{-3'}K_4/K_{BH} = 4.6 \times 10^{-7}$ M^{-1} s^{-1} (Table III), which is some 10^6 smaller than the observed rate constant for acetate catalysis of $k_B = 3.6 \times 10^{-1}$ M^{-1} s^{-1} (Table II). This means that when acetic acid begins to protonate R^-, the cleavage reaction occurs much faster than protonation. It appears that partial proton transfer is sufficient to cause R^- to fall apart into acetaldehyde and ROH.

As in the case of the acid-catalyzed reaction, the observed catalysis is much larger than can be accounted for by simple hydrogen bonding, which suggests that proton transfer is playing an active role in driving the reaction. Hydrogen bonding of the base catalyst to the positive charge of the dipolar hydrate $R^{\pm}$ gives a ratio $k_{Ac}/55.5k_w = 0.2$ M^{-1}, from eq 4 and $pK_3 = 1.0$ for $R^{\pm}$ (Table III). This ratio is much smaller than the observed value of $k_{Ac}/55.5k_w = 40$ M^{-1} for cleavage of the hydrate (Table II). The calculated maximum value of β from eq 4 is 0.20 for hydrogen bonding, which is much smaller than the observed value of $\beta = 0.39$. Thus, simple hydrogen bonding of the base catalyst to the proton on the attacking water molecule could account for only a very small fraction of the observed catalysis. We conclude that concerted proton transfer to the base in the transition state plays an active role in the reaction; in the addition direction it increases the nucleophilicity of the attacking water molecule and traps the addition intermediate; in the reverse direction proton donation to the leaving oxygen atom withdraws electrons from carbon and provides the driving force for cleavage of the C–O bond.

The absolute values of the rate constants for the individual steps of the class n mechanism are generally reasonable (Table III), with the exception of the water-catalyzed reaction. The calculated rate constant k_4 for deprotonation of acetaldehyde hydrate by water to form R^-, which represents rate-limiting diffusional separation of the $R^-{\cdot}H_3O^+$ complex, is 19-fold slower than the observed rate constant k_w; in the reverse direction the calculated rate constant k_{BH} for reaction of H_3O^+ with R^- to give products is slightly above the diffusion-controlled limit. These problems may be avoided by a "one-encounter" mechanism in which the initially formed H_3O^+ donates a proton to R^- before it diffuses away, so that the diffusional steps are avoided. On the other hand, the alternative class e mechanism (k_A, Figure 4) would require a value of $k_A = 10^{15}$ M^{-1} s^{-1} for the reaction of hydroxide ion with R^+ (Table III); this is far above the diffusion-controlled limit and excludes this mechanism for the water reaction.

The rate constants for the water reaction are close to those expected from the Brønsted plots for general base catalysis by a class n mechanism (Figure 9), which suggests that the water reaction follows this mechanism; they are 100–60000 times larger than predicted by the Brønsted plots for general acid catalysis by a class e mechanism. The absence of significant positive deviations of the rate constants for the water reaction from the Brønsted plots for general base catalysis shows that there is no significant rate acceleration from a concerted cyclic mechanism involving proton transfer through water in the rate-limiting step.

Catalysis by Hydroxide Ion. The rate constants for catalysis by hydroxide ion show positive deviations from the Brønsted plots for general base catalysis, although the deviations are smaller than those for the formaldehyde reactions.[7] This suggests that these reactions proceed through a different mechanism, which involves specific base catalysis (eq 11). The rate constants for catalysis by hydroxide ion do not fit the correlation with eq 7 that describes

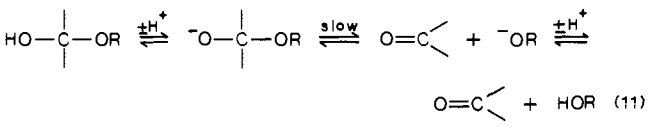

(11)

the data for other catalysts (Figures 7, 11, 12 and 14), and the ratios of the rate constants for hydroxide ion catalysis of the acetaldehyde and formaldehyde reactions do not show the decrease with increasing pK_a of the alcohol that is characteristic of concerted class n catalysis by weaker bases (Figure 14).

The class n mechanism is not expected for hydroxide ion catalysis because there is no thermodynamic advantage to protonation of most of the anionic leaving groups by water acting as a general acid catalyst.[59] Extrapolation of the values of β_{lg} for catalysis by buffer bases through the class n mechanism according to eq 6 gives values of β_{lg} ranging from −0.7 to −1.5 for hydroxide ion catalysis of the cleavage of acetaldehyde ethyl and trifluoroethyl hemiacetals, respectively. This results in transition-state locations far outside the diagram of Figure 13, as might be expected if hydroxide ion catalysis occurs by a different mechanism. It shows that there must be a change to a mechanism involving little or no protonation of the leaving group in the transition state with strong bases, at least for the more acidic alcohols. The hydroxide ion catalyzed reaction can be described by a vertical reaction coordinate on the right side of Figure 13A that corresponds to a stepwise mechanism involving C–O bond formation and cleavage with no associated proton transfer (not shown).

The Interpretation of Brønsted Coefficients and Other Structure–Reactivity Parameters. Much of our present understanding of reaction mechanisms is based on the assumption that the structure–reactivity behavior of rate and equilibrium constants, or of transition states and ground states, may be treated in the same way because these states are related by a kind of quasie-quilibrium. However, this assumption and the use of Brønsted α and β values, Hammett slopes, and other structure–reactivity parameters as measures of reaction progress have been questioned.[23,24,48,60] Energy contour diagrams that are defined by structure–reactivity parameters provide a self-consistent description of structure–reactivity parameters and their changes with changing reactant structure.[19,20] It is of interest to consider the extent to which they may also be interpreted in terms of transition-state structure.

If the magnitude of a Brønsted β value, for example, depends on an electrostatic interaction of a polar substituent with a partially developed charge in the transition state and the charge development depends on the amount of proton transfer or bond formation, then the β value is a measure of these processes. For simple bond formation or cleavage the relationship is monotonic. However, polar substituents on central atoms measure changes in charge development that depend on the balance between bond formation and cleavage. One example of this is resonance delocalization to a different group that results in an imblance between σ bond cleavage and π bond formation, as in the ionization of nitroalkanes.[48,49] Central atom effects do not measure reaction progress directly, but they help to characterize the transition state and may measure the relative progress of partial reactions. Comparisons should usually be limited to a reaction series with the same reacting atoms, because different elements may give different charge distributions that are difficult to interpret.[20]

The interpretation of Brønsted α and β values as a measure of proton transfer in complex reactions, such as those considered here, has been questioned because of possible changes in the position and energy of the transition state that may not reflect the amount of proton transfer in the transition state.[23,24] It was suggested, following earlier suggestions,[22,41] that in class n reactions the proton may jump between the catalyst and the alcohol oxygen atoms when the pK_a values of these groups become equal as the C–O bond is formed or cleaved.[61] Changing the energy of one side of the energy diagram for the reaction will change the position of the y coordinate at which $\Delta pK = 0$ and might change the energy of the transition state in a way that does not depend on the position of a transition state along the x axis for proton transfer.

However, it is unlikely that proton transfer occurs in a separate step with no barrier or that it always occurs through a transition

(59) Jencks, W. P. *J. Am. Chem. Soc.* **1972**, *94*, 4731.
(60) Pross, A. *J. Org. Chem.* **1984**, *49*, 1811. Shaik, S. S. *Prog. Phys. Org. Chem.* **1985**, *15*, 198.
(61) Somewhat similar ideas were put forward by Dogonadze and coworkers; see: Ulstrup, J. *Charge Transfer Processes in Condensed Media*; Springer-Verlag: Berlin, Heidelberg, 1979.

state that is located at the same position on the x axis. The published energy diagrams show an energy well or no barrier along the x axis for the proton transfer,[23,24] but it is likely that there is some such barrier[62] because proton transfer between electronegative atoms at $\Delta pK = 0$ is considerably slower than expected for a diffusion-controlled reaction[33] and shows a significant deuterium isotope effect.[63] This barrier may represent proton transfer over a barrier, tunneling through the barrier, and/or motion of the heavy atoms toward each other that decreases the barrier.[22,41,63] The proton transfer may involve tunneling, but tunneling does not require that the proton transfer must occur as a separate step. There is experimental and theoretical support for tunneling in E2 elimination reactions and the mutarotation of tetramethylglucose, which involve concerted transfer of one or more protons and changes in bonding to heavy atoms in the transition state.[64]

The reaction will follow the path of lowest Gibbs energy from reactants to products, which passes through the transition state at a saddle point. If the reaction path does not proceed through the corners of the diagram, the saddle point will ordinarily be located somewhere in the central area of the diagram because of the high energy of the intermediate structures at the corners. We can characterize the ground states of the reaction and the transition state at the saddle point; we do not know the path that is followed to reach the transition state, although it is likely that it is close to the path of steepest descent from the saddle point. The position of the transition state can be defined, within the limits of the uncertainty principle, even if the curvature along the coordinate for proton transfer is zero or negative.

Empirical energy contour diagrams that are defined by structure–reactivity parameters provide a self-consistent description of changes in these parameters with changing reactant structure. Appendix 1 of ref 19 shows that there is a linear relationship between the Brønsted β value, $\partial \log k/\partial pK_{BH}$, and the coordinate for proton transfer at the saddle point, x, when a linear energy perturbation is applied to an energy contour diagram. This conclusion holds for small perturbations regardless of the nature of the energy surface or its edges. The reason for the conclusion is obvious for changes in pK_{BH} (the energy of the right side of Figure 13) when the position of the transition state on the y coordinate is constant because the x coordinate is defined by β, so that the fraction of the perturbation at x is equal to β. The conclusion is less obvious but is still true when the y coordinate of the transition state changes. Consider the case in which the curvatures a and b are equal to zero for energy contour lines that pass through the saddle point parallel to the x and y axes, respectively. The reaction coordinate is then diagonal and the curvatures of the surface perpendicular and parallel to the reaction coordinate at the saddle point are equal but opposite. When $b = 0$ the change in energy of the transition state is independent of the y coordinate of the transition state and $x = \beta$. Appendix 1 shows that this conclusion holds also when the curvatures are not zero.[19] If significant changes in x do occur they will appear as curvature in the observed Brønsted plots.

If proton transfer occurs by tunneling through a barrier the exact position of the proton in the transition state cannot be specified. However, tunneling is likely to take place at an approximately constant distance below the top of the barrier so that the position and movements of the barrier will appear in the observed structure–reactivity behavior. We conclude that energy contour diagrams that are defined by structure–reactivity parameters provide a useful description of the characteristics of a reaction even if tunneling occurs and that they are indicators of reaction progress, to the extent that this can be defined when tunneling is significant.

(62) Lamaty, G., personal communication.
(63) Bergman, N.-A.; Chiang, Y.; Kresge, A. J. *J. Am. Chem. Soc.* **1978**, *100*, 5954. Cox, M. M.; Jencks, W. P. *J. Am. Chem. Soc.* **1978**, *100*, 5956. Fischer, H.; DeCandis, F. X.; Ogden, S. D.; Jencks, W. P. *J. Am. Chem. Soc.* **1980**, *102*, 1340.
(64) Subramanian, R.; Saunders, W. H., Jr. *J. Am. Chem. Soc.* **1984**, *106*, 7887. Saunders, W. H., Jr. *J. Am. Chem. Soc.* **1984**, *106*, 2223. Engdahl, K.-A.; Bivehed, H.; Ahlberg, P.; Saunders, W. H., Jr. *J. Am. Chem. Soc.* **1983**, *105*, 4767.

Thermal [1,7]-Sigmatropic Hydrogen Shifts: Stereochemistry, Kinetics, Isotope Effects, and π-Facial Selectivity[1,2]

Carl A. Hoeger, Allen D. Johnston, and William H. Okamura*

Contribution from the Department of Chemistry, University of California, Riverside, California 92521. *Received January 26, 1987*

Abstract: The antarafacial stereochemistry of the thermal [1,7]-sigmatropic hydrogen shift has been demonstrated. The substrates studied include the epimeric *cis*-isotachysterol analogues **1** and **4** and their stereospecifically 15α-deuterium-labeled derivatives **7** and **10**, respectively. Two different synthetic routes to the key labeled intermediate **23b** are described; the highly stereoselective transformation of **18** to **19** to **20** proved to be a particularly useful observation for expeditious completion of this study and may be useful for *trans*-hydrindane syntheses in general (e.g., in steroid applications). The observations that heating **7** produces only **8** and **9**, and no **8′** and **9′**, and, likewise, that heating **10** produces only **11** and **12**, and no **11′** and **12′**, demonstrate antarafaciality. Kinetic investigations in the temperature range 67–98 °C of the thermal isomerization of unlabeled **1** and **2** reveal that they undergo [1,7]-sigmatropic shifts with activation parameters characteristic of other [1,7]-shifts. The kinetic studies of **1** and **2** also reveal that the configurational orientation of the allylic hydroxyl group exerts a significant syn-π-facial directive effect on the helicity of this antarafacial, pericyclic process. This is just the opposite to the anti-π-facial selectivity previously reported for thermal, suprafacial [1,5]-sigmatropic shifts of allylic hydroxyl substituted systems. Lastly, the kinetic studies of **1** and **2** coupled with those of labeled isomers **4** and **10** reveal primary deuterium kinetic isotope effects (k_H/k_D) of 4.0 and 2.6 [for the processes **1**(**7**) → **3**(**9**) and **4**(**10**) → **6**(**12**), respectively]. These relatively normal kinetic isotope effect values are an order of magnitude smaller than the only other value previously recorded for the thermal [1,7]-sigmatropic hydrogen shift.

The thermal [1,5]- and [1,7]-sigmatropic hydrogen shifts are subsets of pericyclic processes first systematically defined in 1965 by Woodward and Hoffmann[3] (see Chart I). The classic metabolic transformation of previtamin D_3 to vitamin D_3 is a pivotal

0002-7863/87/1509-4690$01.50/0